

# Surface plasma resonance and magneto-optical enhancement in composites containing multicore-shell structured nanoparticles

Masanori Abe and Takeshi Suwa

*Department of Physical Electronics, Tokyo Institute of Technology, Ookayama, Meguro-ku, Tokyo 152-8552, Japan*

(Received 5 April 2004; published 1 December 2004)

We have formulated the conditions in which dipolar surface plasma resonance is excited by light waves in composites containing nanometer-sized,  $n$ -fold multicore-shell structured particles (referred henceforth as “nano-onions”) dispersed in matrices. The nano-onions have ellipsoidal shape and an arbitrary layer number  $n$ , which contain shell(s) (or core) of a metal having Drude type free electrons responsible for the surface plasma oscillation. By solving a quasistatic potential boundary problem in a nano-onion that is exposed to an external static electric field, we derived the effective dielectric permittivity tensor, including off-diagonal elements, for the composites, based on the Maxwell Garnett theory. The results were utilized not only to derive the resonance conditions but also to formulate the surface charge densities on the metal surfaces, from which we determined the symmetry of the dipolar surface plasmon polaritons excited in the metal shells. Calculations made on the composites containing model nano-onions of spherical shape having  $n$ -fold core-shell structure of sodium and a dielectric revealed the following results: (1) The surface plasmon resonance occurs at  $n$  eigenfrequencies, similar to the mechanical oscillation in  $n$ -fold coupled oscillators; (2) at these eigenfrequencies, the composite causes resonant peaks of light extinction coefficient, and (3) the magneto-optical Kerr effect induced by a static external magnetic field is remarkably enhanced at the resonance frequencies. The magneto-optical enhancement is augmented by hypothetically reducing the dielectric loss in Na, thus increasing the quality factor  $Q$  of the surface plasmon resonance. The validity limit in our calculations based on the effective medium approximation by the Maxwell Garnett theory is discussed, comparing with the calculations made by Sinzig and Quinten [Appl. Phys. A **58**, 157 (1994)] based on a rigorous Mie scattering theory treatment.

DOI: 10.1103/PhysRevB.70.235103

PACS number(s): 78.67.-n, 45.70.-n, 78.40.-q, 78.20.-e

## I. INTRODUCTION

In this study we analyzed surface plasma resonance in nanoparticles with multicore-shell structures, and found that the magneto-optical effect is remarkably enhanced near the resonance. Such multifold core-shell structured nanoparticles, referred to here as “nano-onions,”<sup>1</sup> are attracting extensive attention at present, since the multilayered structures are expected to give particular magnetic properties and exhibit unique optical and magneto-optical effects similarly observed in metallic multilayers of nanometer-scale thickness.<sup>2</sup>

Surface plasma (or plasmon) resonance is an excitation of charge density surface waves, which propagate along a metallic surface or on metal films.<sup>3–5</sup> The free electrons, following the Drude theory, play an essential role in surface plasmon resonance, which is most prominently observed in noble and alkaline metals. The surface plasmons can be excited by light waves, making a contrast with volume plasmons that can be excited not by light waves but by electron beams. Therefore, the surface plasmon resonance has attracted special interest among researchers studying optically induced phenomena in matter. They found that the surface plasmon resonance enhances magneto-optical effects,<sup>6–12</sup> nonlinear optical processes,<sup>11–13</sup> surface Raman scatterings,<sup>14–16</sup> and photon-induced catalysis reactions<sup>17</sup> to a remarkable extent. This created much interest not only in solid-state physics but also in sensor technology, because the physical effect enhancements by the surface plasmons facilitated a variety of highly sensitive surface analysis devices, including chemical sensors<sup>18</sup> and biomedical sensors.<sup>19</sup>

Optical excitation of surface plasmons on planar metal surfaces can be realized only by evanescent waves, because surface plasmons have retarded dispersion relations with respect to the excitation light waves.<sup>3–6,9–11,13</sup> However, even using ordinary (nonevanescent) light waves, surface plasmons can be excited on fine metal particles,<sup>7,8,12,14,15,17,20–23</sup> which may be embedded in matrices (thus forming granular composites)<sup>7,12,17,20–23</sup> or located on planar surfaces.<sup>8,14–17,24,25</sup> The particles on the planar surfaces offer a model for rough surfaces on which surface plasmons are excited to enhance the surface Raman scattering.<sup>13–16</sup> Surface plasmon resonance excited by light waves in fine metal particles have therefore been studied extensively.

Granqvist and Hunderi<sup>21</sup> analyzed the optical absorption by ultrafine (3–4 nm in diameter) Ag spheres in terms of surface plasmon resonance. Applying the Maxwell Garnett (MG) theory<sup>26</sup> and the Bruggeman theory,<sup>27</sup> they calculated effective dielectric constants for composites containing the Ag nanoparticles dispersed in matrices based on effective medium approximation. The MG theory presupposes that the particles are sparsely dispersed, or the filling factor of the particles is small, while the Bruggeman theory is free from such a premise on the filling factor, as will be described in Sec. V. Hui and Stroud<sup>7</sup> showed using the MG theory that magneto-optical Faraday rotation in dilute suspension of small particles of a Drude metal is enhanced by the surface plasma resonance on the metal surfaces. The analyses were extended to higher concentrations of the suspensions by applying the Bruggeman theory.<sup>23</sup> The analyses of surface plasmon based on the MG theory were further extended to such

core/shell structured nanoparticles as Ag spheres having inner dielectric cores<sup>28</sup> or outer dielectric shells,<sup>29</sup> with which they explained the optical absorption and the surface-enhanced Raman scattering by the plasma resonance in the Ag shells or the cores.

Almost a century ago, Mie<sup>30</sup> showed with his scattering theory that spherical metal particles exhibit resonant extinction of light, which was later interpreted by Kreibig *et al.*<sup>20,31,32</sup> by the concept of electric and magnetic multipolar excitations due to surface plasmon polaritons and eddy currents, respectively. They revealed, based on the Mie theory, that the resonant light absorption observed for spherical nanoparticles of Ag and Au can be interpreted by invoking the surface plasma resonance of electric multipolar modes, mainly from the lowest electric excitation mode called the dipolar surface plasmon polariton mode. From the Mie scattering theory, Kerker *et al.*<sup>33</sup> and Messinger *et al.*<sup>34</sup> explained the surface enhanced Raman scattering in spherical metal particles in terms of surface plasmon resonance. Wokaun<sup>35</sup> extended the Mie formalism for the surface plasmon resonance to spheroidal metal particles, with which he investigated the marked surface enhancements of Raman scattering and the catalytic activity of the Ag nanoparticles. The Mie theory analyses on the surface plasmon resonance were further extended to the double layered nanoparticles having spherical dielectric (core)/Ag (shell),<sup>36</sup> spheroidal latex (core)/Ag (shell),<sup>37</sup> and spherical Au (core)/Pt (shell)<sup>38</sup> structures.

Sinzig and Quinten<sup>39</sup> investigated the surface plasmon resonance in  $n$ -fold multi-core-shell structured particles with arbitrary number  $n$ . Calculating the Mie scattering intensities, they showed that the multicore-shell structures with alternate stratification of Na and a dielectric exhibit resonant peaks of light extinction, which they guessed to be ascribed to the surface plasmon polaritons excited in the Na shells and cores. They also proposed that in the core(dielectric)/shell(metal) structured ( $n=2$ ) particles embedded in a dielectric matrix, two surface plasmon eigenmodes are excited, having symmetric and anti-symmetric charge distributions, respectively, on the inner and outer surfaces of the metal shell. Their calculations were, however, not derived analytically, but from analogy with the surface plasmon eigenmodes excited in a metal planar layer. By the Mie scattering theory they calculated the fields induced in and scattered outside the particles, using complicated recurrent formulas; the Mie scattering theory cannot give analytical expressions for the fields or, therefore, the conditions in which surface plasmon resonance occurs.

In this study we derived, based on the MG theory, analytical formulas for the fields induced in the  $n$ -fold nano-onions, and formulated the conditions in which the surface plasmon resonance takes place in the composites containing the nano-onions. We also formulated the charge distributions induced on the surfaces of the metal shells, with which we determined the symmetry of the surface plasmon polariton eigenmodes induced in the metal shells. We revealed that the surface plasmon resonance enhances not only light extinction but also magneto-optical effects. In our calculations we assumed that the nano-onions much smaller than the light wavelength are dispersed sparsely in a dielectric matrix to

form a composite. The light waves propagate in such a composite as if it were a continuous medium, called an “effective medium,” having an “effective dielectric permittivity.” We derived the effective permittivity based on the MG theory in tensor form, including the off-diagonal terms that are responsible for the magneto-optical effects.

The effective dielectric permittivity tensor was derived by Lissberger and Saunders<sup>40</sup> based on the MG theory in order to explain the magneto-optical Kerr effect for cermets, or composites in which magnetized spherical particles are embedded in dielectric materials. Carey *et al.*<sup>41</sup> extended the effective dielectric tensor to spherical particles with a core/shell structure, thus explaining the magneto-optical effects in granular films in which surface-oxidized Co particles are dispersed in a dielectric matrix. Abe,<sup>42</sup> one of the authors of this paper, generalized the effective dielectric permittivity tensor to composites containing magnetized, oriented ellipsoid particles embedded in matrices which may be magnetic or non-magnetic. The effective dielectric tensor will be further extended in this study to the nano-onions having an arbitrary number of core/shell layers.

In Sec. II, we will solve a quasistatic potential boundary problem for the electric fields induced in the core and shells of a magnetized  $n$ -fold nano-onion in order to derive the electric polarizability of the nano-onion. The result will be used to formulate, based on the MG theory, the effective dielectric permittivity tensor for composites containing the magnetized nano-onions. In Sec. III, we will derive the conditions upon which the surface plasmon resonance occurs in the composites, and derive an equation that we can use to determine the symmetry of the charge distributions of surface plasmon polariton eigenmodes. In Sec. IV, we will investigate the resonant conditions for the surface plasmons in a composite containing the spherical,  $n$ -fold nano-onions made of Na and a dielectric. It will be shown that the magneto-optical Kerr effect, as well as the light extinction, is remarkably enhanced by the surface plasmon oscillation. In Sec. V, we will discuss the applicability limits in the MG theory and then conclude.

## II. DERIVATION OF EFFECTIVE DIELECTRIC TENSOR

### A. Potential boundary problem

In order to derive the effective dielectric permittivity tensor based on the MG theory for the composites containing ellipsoidal nano-onions (Fig. 1) we first solve the potential boundary problem for the electric fields induced in the core and shells of a magnetized nano-onion that is embedded in a matrix. Using the quasistatic approximation, we neglect the spatial dependence of the electric field of the light, but the time dependence is introduced through the wavelength dependent complex dielectric functions for the core and the shells.

Consider that a uniform, isotropic medium has in it a uniform, or quasistatic electric field

$$\mathbf{F}_0 = \begin{bmatrix} F_0^x \\ F_0^y \\ F_0^z \end{bmatrix}. \quad (2.1)$$

Let a nano-onion, ellipsoidal in shape (which is generalized from spheroidal in our previous study<sup>42</sup>), be embedded in the

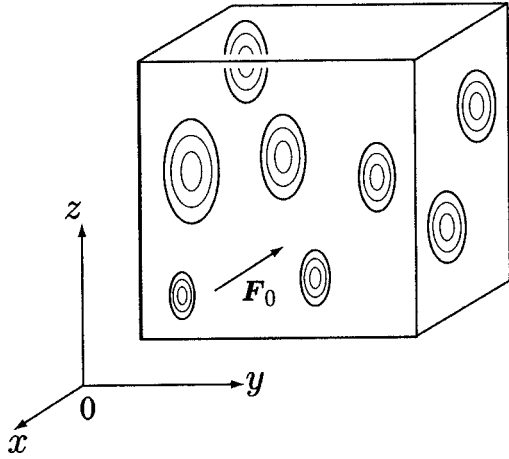


FIG. 1. A composite containing an oriented, spatially random array of ellipsoidal nano-unions embedded in a host material in which a uniform magnetic field  $\mathbf{F}_0$  exists.

matrix (numbered as  $m=0$ ), as shown in Fig. 2. The outermost surface of each nano-ion has principal radii of  $a$ ,  $b$ , and  $c$ , along which we define the  $x$ ,  $y$ , and  $z$  axes, respectively. The nano-ion has a co-centric,  $n$ -fold core/shell structure whose boundaries are expressed by the following quadratic equations:

$$\frac{x^2}{a_m^2} + \frac{y^2}{b_m^2} + \frac{z^2}{c_m^2} = 1 \quad (m = 1, 2, \dots, n). \quad (2.2)$$

Here,  $a_m$ ,  $b_m$ , and  $c_m$  are the principal radii of the outer surface of the  $m$ th shell or the core ( $m=n$ ), and thus

$$a_1 = a, \quad b_1 = b, \quad c_1 = c. \quad (2.3)$$

Now, we introduce ellipsoidal coordinates  $\xi$ ,  $\eta$ , and  $\zeta$  as follows:<sup>43</sup>

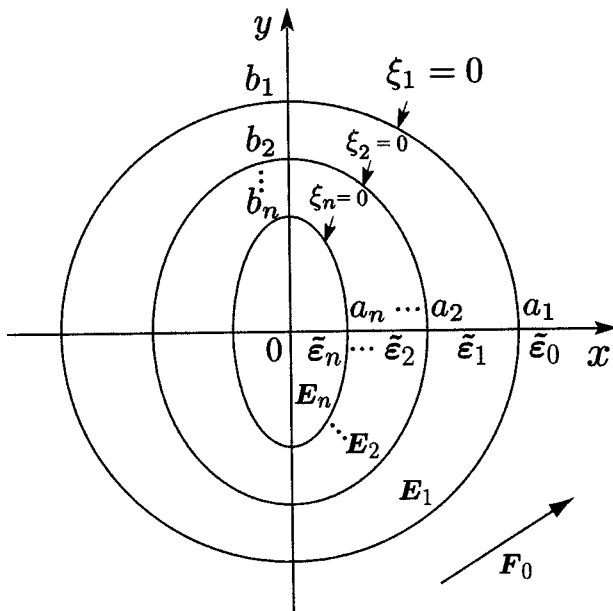


FIG. 2. Cross section in  $xy$  plane for an  $n$ -fold nano-ion.

$$x = \pm \{(\xi + a^2)(\eta + a^2)(\zeta + a^2)\}^{1/2} / \{(b^2 - a^2)(c^2 - a^2)\}^{1/2}, \quad (2.4a)$$

$$y = \pm \{(\xi + b^2)(\eta + b^2)(\zeta + b^2)\}^{1/2} / \{(c^2 - b^2)(a^2 - b^2)\}^{1/2}, \quad (2.4b)$$

$$z = \pm \{(\xi + c^2)(\eta + c^2)(\zeta + c^2)\}^{1/2} / \{(a^2 - c^2)(b^2 - c^2)\}^{1/2}, \quad (2.4c)$$

which are valid in the ranges, satisfy the following relations:

$$-c'^2 \leq \xi, \quad -b'^2 \leq \eta \leq -c'^2, \quad -a'^2 \leq \zeta \leq -b'^2. \quad (2.5a)$$

In this equation,  $a'$ ,  $b'$ , and  $c'$  represent the maximum, mid-point, and minimum values of  $a$ ,  $b$ , and  $c$ , respectively, that satisfy the relationship

$$c' < b' < a'. \quad (2.5b)$$

Using the radial coordinate  $\xi$ , the outer boundary of the  $m$ th medium is expressed by

$$\xi = \xi_m \quad (m = 1, 2, 3, \dots, n), \quad (2.6a)$$

where

$$\xi_1 = 0, \quad (2.6b)$$

and  $\xi_m$ 's satisfy the following equations:

$$a_m = (\xi_m + a^2)^{1/2}, \quad (2.7a)$$

$$b_m = (\xi_m + b^2)^{1/2}, \quad (2.7b)$$

$$c_m = (\xi_m + c^2)^{1/2}, \quad (2.7c)$$

$$(m = 1, 2, \dots, n).$$

It should be noted that  $a_m : b_m : c_m$  depends on  $m$ , and, therefore, the boundary surfaces are not of similar shape, that is, the further out the more spherical in shape is the shell.

Let the nano-unions and the matrix be magnetized along an arbitrary direction, and express the dielectric permittivity tensor  $\tilde{\epsilon}_m$  for the  $m$ th medium to the first order of magnetization as follows:

$$\tilde{\epsilon}_m = \begin{bmatrix} \epsilon_m & \epsilon_m^{xy} & \epsilon_m^{xz} \\ \epsilon_m^{yx} & \epsilon_m & \epsilon_m^{yz} \\ \epsilon_m^{zx} & \epsilon_m^{zy} & \epsilon_m \end{bmatrix} \quad (m = 0, 1, 2, \dots, n), \quad (2.8a)$$

$$\epsilon_m^{xy} + \epsilon_m^{yx} = \epsilon_m^{yz} + \epsilon_m^{zy} = \epsilon_m^{zx} + \epsilon_m^{xz} = 0. \quad (2.8b)$$

Our task is to obtain the electric field

$$\mathbf{E}_m = \begin{bmatrix} E_m^x \\ E_m^y \\ E_m^z \end{bmatrix} \quad (m = 0, 1, 2, \dots, n), \quad (2.9)$$

which is induced in the  $m$ th medium. The electric flux density in the  $m$ th medium

$$\mathbf{D}_m = \begin{bmatrix} D_m^x \\ D_m^y \\ D_m^z \end{bmatrix} \quad (m = 0, 1, 2, \dots, n) \quad (2.10)$$

is given by the product of  $\tilde{\mathbf{e}}_m$  and  $\mathbf{E}_m$  as

$$\mathbf{D}_m = \tilde{\mathbf{e}}_m \mathbf{E}_m. \quad (2.11)$$

The external field  $\mathbf{F}_0$  is no longer equal to  $\mathbf{E}_0$  in the matrix or  $\mathbf{E}_m$  ( $m \geq 1$ ) in the shells or core, because  $\mathbf{F}_0$  induces electric dipole moments inside the nano-onion. Now we assume that in the shells and core, uniform electric fields

$$\mathbf{F}_m = \begin{bmatrix} F_m^x \\ F_m^y \\ F_m^z \end{bmatrix} \quad (m = 1, 2, \dots, n) \quad (2.12)$$

exist and uniform polarizations

$$\mathbf{P}_m = \begin{bmatrix} P_m^x \\ P_m^y \\ P_m^z \end{bmatrix} \quad (m = 1, 2, \dots, n) \quad (2.13)$$

are induced in the nano-onion with respect to the matrix. We express  $\mathbf{E}_m$  in terms of electric field potential  $\phi_m$  to the form

$$\mathbf{E}_m = -\nabla \phi_m \quad (m = 0, 1, 2, \dots, n), \quad (2.14a)$$

$$\begin{aligned} \phi_m = & -\{F_m^x + C_m^x A^x(\xi)\}x - \{F_m^y + C_m^y A^y(\xi)\}y \\ & - \{F_m^z + C_m^z A^z(\xi)\}z \end{aligned} \quad (2.14b)$$

$$= -\sum_i E_m^i u^i \quad (m = 0, 1, 2, \dots, n), \quad (2.14c)$$

$$E_m^i = F_m^i + C_m^i A^i(\xi) \quad (i = x, y, z; m = 0, 1, 2, \dots, n). \quad (2.14d)$$

Here, we rewrote  $x$ ,  $y$ , and  $z$  as  $u^i$  ( $i=x, y, z$ ), i.e.,

$$u^x = x, \quad u^y = y, \quad u^z = z, \quad (2.15)$$

and expressed the  $i$ th component of the dipole field in the  $m$ th medium as  $C_m^i A^i(\xi)$ , with  $A^i(\xi)$  given by<sup>43,44</sup>

$$A^x(\xi) = \int_{\xi}^{\infty} (s+a^2)^{-3/2} (s+b^2)^{-1/2} (s+c^2)^{-1/2} ds, \quad (2.16a)$$

$$A^y(\xi) = \int_{\xi}^{\infty} (s+b^2)^{-3/2} (s+c^2)^{-1/2} (s+a^2)^{-1/2} ds, \quad (2.16b)$$

$$A^z(\xi) = \int_{\xi}^{\infty} (s+c^2)^{-3/2} (s+a^2)^{-1/2} (s+b^2)^{-1/2} ds. \quad (2.16c)$$

Note that the dipole field is not induced in the core; namely,

$$C_n^x = C_n^y = C_n^z = 0, \quad (2.17)$$

because the core has no inner structure.

In the ellipsoidal coordinate system,  $\mathbf{E}_m$  is expressed in terms of  $\phi_m$  as

$$\mathbf{E}_m = \begin{pmatrix} E_m^{\xi} \\ E_m^{\eta} \\ E_m^{\zeta} \end{pmatrix} = \begin{pmatrix} -h_1^{-1} \partial \phi_m / \partial \xi \\ -h_2^{-1} \partial \phi_m / \partial \eta \\ -h_3^{-1} \partial \phi_m / \partial \zeta \end{pmatrix} \quad (m = 0, 1, 2, \dots, n), \quad (2.18)$$

where  $h_1$ ,  $h_2$ , and  $h_3$  are metrical coefficients,<sup>44</sup> and  $\mathbf{D}_m$  is related to  $\mathbf{E}_m$  by

$$\mathbf{D}_m = \begin{bmatrix} D_m^{\xi} \\ D_m^{\eta} \\ D_m^{\zeta} \end{bmatrix} = \begin{bmatrix} \varepsilon_m^{\xi\xi} & \varepsilon_m^{\xi\eta} & \varepsilon_m^{\xi\zeta} \\ \varepsilon_m^{\eta\xi} & \varepsilon_m^{\eta\eta} & \varepsilon_m^{\eta\zeta} \\ \varepsilon_m^{\zeta\xi} & \varepsilon_m^{\zeta\eta} & \varepsilon_m^{\zeta\zeta} \end{bmatrix} \begin{bmatrix} E_m^{\xi} \\ E_m^{\eta} \\ E_m^{\zeta} \end{bmatrix} \quad (m = 0, 1, 2, \dots, n). \quad (2.19)$$

On the  $m$ th ellipsoidal surface,  $\mathbf{E}_m$  and  $\mathbf{D}_m$  must satisfy the following boundary conditions:<sup>43,44</sup>

$$(E_m^{\eta})_{\xi=\xi_m} = (E_{m-1}^{\eta})_{\xi=\xi_m} \quad (m = 1, 2, \dots, n), \quad (2.20a)$$

$$(E_m^{\xi})_{\xi=\xi_m} = (E_{m-1}^{\xi})_{\xi=\xi_m} \quad (m = 1, 2, \dots, n), \quad (2.20b)$$

$$(D_m^{\xi})_{\xi=\xi_m} = (D_{m-1}^{\xi})_{\xi=\xi_m} \quad (m = 1, 2, \dots, n). \quad (2.20c)$$

As shown in the Appendix, we derive from Eq. (2.20) the following recurrent vector formula:

$$\begin{aligned} \varepsilon_{m-1} \mathbf{F}_{m-1} = & \{\tilde{\mathbf{N}}_m (\tilde{\mathbf{e}}_m - \tilde{\mathbf{e}}_{m-1}) + \varepsilon_{m-1} \tilde{\mathbf{1}}\} \mathbf{F}_m + \beta_m \tilde{\mathbf{N}}_m \{(\tilde{\mathbf{e}}_m - \tilde{\mathbf{e}}_{m-1}) \\ & \times \tilde{\mathbf{N}}_m - (\varepsilon_m - \varepsilon_{m-1}) \tilde{\mathbf{1}}\} \mathbf{C}_m \end{aligned} \quad (2.21)$$

$$\begin{aligned} -\beta_m \varepsilon_{m-1} \mathbf{C}_{m-1} = & (\tilde{\mathbf{e}}_m - \tilde{\mathbf{e}}_{m-1}) \mathbf{F}_m \\ & + \beta_m \{(\tilde{\mathbf{e}}_m - \tilde{\mathbf{e}}_{m-1}) \tilde{\mathbf{N}}_m - \varepsilon_m \tilde{\mathbf{1}}\} \mathbf{C}_m. \end{aligned} \quad (2.22)$$

Here we rewrote  $C_m^i$  ( $i=x, y, z$ ) in a vector form, as

$$\mathbf{C}_m = \begin{bmatrix} C_m^x \\ C_m^y \\ C_m^z \end{bmatrix}, \quad (2.23)$$

and put

$$\tilde{\mathbf{1}} = \begin{bmatrix} 1 & 0 & 0 \\ 0 & 1 & 0 \\ 0 & 0 & 1 \end{bmatrix}, \quad (2.24)$$

$$\tilde{\mathbf{N}}_m = \begin{bmatrix} N_m^x & 0 & 0 \\ 0 & N_m^y & 0 \\ 0 & 0 & N_m^z \end{bmatrix} \quad (m = 1, 2, \dots, n), \quad (2.25)$$

$$N_m^i = A^i(0) a_m b_m c_m / 2 \quad (i = x, y, z; m = 1, 2, \dots, n), \quad (2.26)$$

$$\beta_m = 2abc/a_m b_m c_m \quad (m = 1, 2, \dots, n), \quad (2.27)$$

where  $N_m^i$  is the depolarization factor along the  $i$ th axis for the  $m$ th shell (core) and  $\beta_m$  is a constant inversely proportional to the volume inside the  $m$ th boundary surface.

The recurrent relations expressed by Eqs. (2.21) and (2.22) can be rewritten to the form

$$\begin{bmatrix} \mathbf{F}_{m-1} \\ \mathbf{C}_{m-1} \end{bmatrix} = [\tilde{\mathbf{T}}_m] \begin{bmatrix} \mathbf{F}_m \\ \mathbf{C}_m \end{bmatrix} \quad (m = 1, 2, \dots, n), \quad (2.28)$$

where  $[\tilde{\mathbf{T}}_m]$  is a ‘‘super matrix’’ whose components are given by the following matrices:

$$[\tilde{\mathbf{T}}_m] = \begin{bmatrix} \tilde{\mathbf{A}}_m & \tilde{\mathbf{B}}_m \\ \tilde{\mathbf{C}}_m & \tilde{\mathbf{D}}_m \end{bmatrix} \quad (m = 1, 2, \dots, n), \quad (2.29)$$

$$\tilde{\mathbf{A}}_m = \varepsilon_{m-1}^{-1} \{ \tilde{\mathbf{N}}_m (\tilde{\varepsilon}_m - \tilde{\varepsilon}_{m-1}) + \varepsilon_{m-1} \tilde{\mathbf{I}} \}, \quad (2.30a)$$

$$\tilde{\mathbf{B}}_m = \beta_m \varepsilon_{m-1}^{-1} \tilde{\mathbf{N}}_m \{ (\tilde{\varepsilon}_m - \tilde{\varepsilon}_{m-1}) \tilde{\mathbf{N}}_m - (\varepsilon_m - \varepsilon_{m-1}) \tilde{\mathbf{I}} \}, \quad (2.30b)$$

$$\tilde{\mathbf{C}}_m = \beta_m^{-1} \varepsilon_{m-1}^{-1} \{ -(\tilde{\varepsilon}_m - \tilde{\varepsilon}_{m-1}) \}, \quad (2.30c)$$

$$\tilde{\mathbf{D}}_m = \varepsilon_{m-1}^{-1} \{ -(\tilde{\varepsilon}_m - \tilde{\varepsilon}_{m-1}) \tilde{\mathbf{N}}_m + \varepsilon_m \tilde{\mathbf{I}} \}. \quad (2.30d)$$

They are expressed as

$$\tilde{\mathbf{A}}_m = \varepsilon_{m-1}^{-1} \begin{bmatrix} N_m^x (\varepsilon_m - \varepsilon_{m-1}) + \varepsilon_{m-1} & N_m^x (\varepsilon_m^{xy} - \varepsilon_{m-1}^{xy}) & N_m^x (\varepsilon_m^{xz} - \varepsilon_{m-1}^{xz}) \\ N_m^y (\varepsilon_m^{yx} - \varepsilon_{m-1}^{yx}) & N_m^y (\varepsilon_m - \varepsilon_{m-1}) + \varepsilon_{m-1} & N_m^y (\varepsilon_m^{yz} - \varepsilon_{m-1}^{yz}) \\ N_m^z (\varepsilon_m^{zx} - \varepsilon_{m-1}^{zx}) & N_m^z (\varepsilon_m^{zy} - \varepsilon_{m-1}^{zy}) & N_m^z (\varepsilon_m - \varepsilon_{m-1}) + \varepsilon_{m-1} \end{bmatrix}, \quad (2.31a)$$

$$\tilde{\mathbf{B}}_m = \beta_m \varepsilon_{m-1}^{-1} \begin{bmatrix} N_m^x (N_m^x - 1) (\varepsilon_m - \varepsilon_{m-1}) & N_m^x N_m^y (\varepsilon_m^{xy} - \varepsilon_{m-1}^{xy}) & N_m^x N_m^z (\varepsilon_m^{xz} - \varepsilon_{m-1}^{xz}) \\ N_m^y N_m^x (\varepsilon_m^{yx} - \varepsilon_{m-1}^{yx}) & N_m^y (N_m^y - 1) (\varepsilon_m - \varepsilon_{m-1}) & N_m^y N_m^z (\varepsilon_m^{yz} - \varepsilon_{m-1}^{yz}) \\ N_m^z N_m^x (\varepsilon_m^{zx} - \varepsilon_{m-1}^{zx}) & N_m^z N_m^y (\varepsilon_m^{zy} - \varepsilon_{m-1}^{zy}) & N_m^z (N_m^z - 1) (\varepsilon_m - \varepsilon_{m-1}) \end{bmatrix}, \quad (2.31b)$$

$$\tilde{\mathbf{C}}_m = \beta_m^{-1} \varepsilon_{m-1}^{-1} \begin{bmatrix} -(\varepsilon_m - \varepsilon_{m-1}) & -(\varepsilon_m^{xy} - \varepsilon_{m-1}^{xy}) & -(\varepsilon_m^{xz} - \varepsilon_{m-1}^{xz}) \\ -(\varepsilon_m^{yx} - \varepsilon_{m-1}^{yx}) & -(\varepsilon_m - \varepsilon_{m-1}) & -(\varepsilon_m^{yz} - \varepsilon_{m-1}^{yz}) \\ -(\varepsilon_m^{zx} - \varepsilon_{m-1}^{zx}) & -(\varepsilon_m^{zy} - \varepsilon_{m-1}^{zy}) & -(\varepsilon_m - \varepsilon_{m-1}) \end{bmatrix}, \quad (2.31c)$$

$$\tilde{\mathbf{D}}_m = \varepsilon_{m-1}^{-1} \begin{bmatrix} -N_m^x (\varepsilon_m - \varepsilon_{m-1}) + \varepsilon_m & -N_m^y (\varepsilon_m^{xy} - \varepsilon_{m-1}^{xy}) & -N_m^z (\varepsilon_m^{xz} - \varepsilon_{m-1}^{xz}) \\ -N_m^x (\varepsilon_m^{yx} - \varepsilon_{m-1}^{yx}) & -N_m^y (\varepsilon_m - \varepsilon_{m-1}) + \varepsilon_m & -N_m^z (\varepsilon_m^{yz} - \varepsilon_{m-1}^{yz}) \\ -N_m^x (\varepsilon_m^{zx} - \varepsilon_{m-1}^{zx}) & -N_m^y (\varepsilon_m^{zy} - \varepsilon_{m-1}^{zy}) & -N_m^z (\varepsilon_m - \varepsilon_{m-1}) + \varepsilon_m \end{bmatrix}. \quad (2.31d)$$

## B. Polarizability of a nano-onion

In order to derive the polarizability for the nano-onion, let us express  $\mathbf{F}_m$  in terms of  $\mathbf{F}_0$ . Substituting Eq. (2.17) into Eq. (2.28), we obtain

$$\begin{bmatrix} \mathbf{F}_m \\ \mathbf{C}_m \end{bmatrix} = [\tilde{\mathbf{T}}_{m+1}] [\tilde{\mathbf{T}}_{m+2}] \cdots [\tilde{\mathbf{T}}_n] \begin{bmatrix} \mathbf{F}_n \\ \mathbf{0} \end{bmatrix} \quad (m = 1, 2, \dots, n-1), \quad (2.32a)$$

$$\begin{bmatrix} \mathbf{F}_0 \\ \mathbf{C}_0 \end{bmatrix} = [\tilde{\mathbf{T}}_1] [\tilde{\mathbf{T}}_2] \cdots [\tilde{\mathbf{T}}_n] \begin{bmatrix} \mathbf{F}_n \\ \mathbf{0} \end{bmatrix}, \quad (2.32b)$$

where  $\mathbf{0}$  expresses the matrix having only zero components, and thus we obtain

$$\mathbf{F}_m = \{ [\tilde{\mathbf{T}}_{m+1}] [\tilde{\mathbf{T}}_{m+2}] \cdots [\tilde{\mathbf{T}}_n] \}_{1,1} \mathbf{F}_n, \quad (2.33a)$$

$$\mathbf{F}_0 = \{ [\tilde{\mathbf{T}}_1] [\tilde{\mathbf{T}}_2] \cdots [\tilde{\mathbf{T}}_n] \}_{1,1} \mathbf{F}_n. \quad (2.33b)$$

Here  $\{\cdots\}_{1,1}$  designates the first row first column components of the super matrix. Combination of Eqs. (2.33a) and (2.33b) results in

$$\mathbf{F}_m = \{ [\tilde{\mathbf{T}}_{m+1}] [\tilde{\mathbf{T}}_{m+2}] \cdots [\tilde{\mathbf{T}}_n] \}_{1,1} \{ [\tilde{\mathbf{T}}_1] [\tilde{\mathbf{T}}_2] \cdots [\tilde{\mathbf{T}}_n] \}_{1,1}^{-1} \mathbf{F}_0. \quad (2.34)$$

Thus the matrix  $\tilde{\mathbf{S}}_m$ , which connects  $\mathbf{F}_0$  to  $\mathbf{F}_m$  by

$$\mathbf{F}_m = \tilde{\mathbf{S}}_m \mathbf{F}_0 \quad (m = 1, 2, \dots, n), \quad (2.35)$$

is expressed as

$$\tilde{\mathbf{S}}_m = \{[\tilde{\mathbf{T}}_{m+1}][\tilde{\mathbf{T}}_{m+2}] \cdots [\tilde{\mathbf{T}}_n]\}_{1,1} \{[\tilde{\mathbf{T}}_1][\tilde{\mathbf{T}}_2] \cdots [\tilde{\mathbf{T}}_n]\}_{1,1}^{-1}. \quad (2.36)$$

Some of  $\tilde{\mathbf{S}}_m$ 's are given as follows:  
 $n=1$  (nonstructured):

$$\mathbf{S}_1 = \{[\tilde{\mathbf{T}}_1]\}_{1,1}^{-1} = \tilde{\mathbf{A}}_1^{-1}; \quad (2.37)$$

$n=2$  (core/shell structured):

$$\tilde{\mathbf{S}}_1 = \{[\tilde{\mathbf{T}}_2]\}_{1,1} \{[\tilde{\mathbf{T}}_1][\tilde{\mathbf{T}}_2]\}_{1,1}^{-1} = \tilde{\mathbf{A}}_2(\tilde{\mathbf{A}}_1\tilde{\mathbf{A}}_2 + \tilde{\mathbf{B}}_1\tilde{\mathbf{C}}_2)^{-1}, \quad (2.38a)$$

$$\tilde{\mathbf{S}}_2 = \{[\tilde{\mathbf{T}}_1][\tilde{\mathbf{T}}_2]\}_{1,1}^{-1} = (\tilde{\mathbf{A}}_1\tilde{\mathbf{A}}_2 + \tilde{\mathbf{B}}_1\tilde{\mathbf{C}}_2)^{-1}; \quad (2.38b)$$

$n=3$  (core/inner-shell/outer-shell structured):

$$\begin{aligned} \tilde{\mathbf{S}}_1 &= \{[\tilde{\mathbf{T}}_2][\tilde{\mathbf{T}}_3]\}_{1,1} \{[\tilde{\mathbf{T}}_1][\tilde{\mathbf{T}}_2][\tilde{\mathbf{T}}_3]\}_{1,1}^{-1} \\ &= (\tilde{\mathbf{A}}_2\tilde{\mathbf{A}}_3 + \tilde{\mathbf{B}}_2\tilde{\mathbf{C}}_3) \{ \tilde{\mathbf{A}}_1(\tilde{\mathbf{A}}_2\tilde{\mathbf{A}}_3 + \tilde{\mathbf{B}}_2\tilde{\mathbf{C}}_3) \\ &\quad + \tilde{\mathbf{B}}_1(\tilde{\mathbf{C}}_2\tilde{\mathbf{A}}_3 + \tilde{\mathbf{D}}_2\tilde{\mathbf{C}}_3) \}^{-1}, \end{aligned} \quad (2.39a)$$

$$\begin{aligned} \tilde{\mathbf{S}}_2 &= [\tilde{\mathbf{T}}_3]_{1,1} \{[\tilde{\mathbf{T}}_1][\tilde{\mathbf{T}}_2][\tilde{\mathbf{T}}_3]\}_{1,1}^{-1} \\ &= \tilde{\mathbf{A}}_3 \{ \tilde{\mathbf{A}}_1(\tilde{\mathbf{A}}_2\tilde{\mathbf{A}}_3 + \tilde{\mathbf{B}}_2\tilde{\mathbf{C}}_3) + \tilde{\mathbf{B}}_1(\tilde{\mathbf{C}}_2\tilde{\mathbf{A}}_3 + \tilde{\mathbf{D}}_2\tilde{\mathbf{C}}_3) \}^{-1} \end{aligned} \quad (2.39b)$$

$$\begin{aligned} \tilde{\mathbf{S}}_3 &= \{[\tilde{\mathbf{T}}_1][\tilde{\mathbf{T}}_2][\tilde{\mathbf{T}}_3]\}_{1,1}^{-1} \\ &= \{ \tilde{\mathbf{A}}_1(\tilde{\mathbf{A}}_2\tilde{\mathbf{A}}_3 + \tilde{\mathbf{B}}_2\tilde{\mathbf{C}}_3) + \tilde{\mathbf{B}}_1(\tilde{\mathbf{C}}_2\tilde{\mathbf{A}}_3 + \tilde{\mathbf{D}}_2\tilde{\mathbf{C}}_3) \}^{-1}. \end{aligned} \quad (2.39c)$$

The polarization  $\mathbf{P}_m$  [cf. Eq. (2.13)] that is induced in the  $m$ th medium with respect to the matrix having  $\tilde{\epsilon}_0$ , satisfies the relation

$$\tilde{\epsilon}_m \mathbf{F}_m = \tilde{\epsilon}_0 \mathbf{F}_m + \mathbf{P}_m \quad (m = 1, 2, \dots, n). \quad (2.40)$$

Summing up all the  $\mathbf{P}_m$ 's given by Eq. (2.40), the total polarization induced in the nano-ion amounts to

$$\langle \mathbf{P} \rangle = \left( \sum_{m=1}^n V_m \mathbf{P}_m \right) / V_o = \sum_{m=1}^n t_m (\tilde{\epsilon}_m - \tilde{\epsilon}_0) \mathbf{F}_m. \quad (2.41)$$

Here we introduced  $t_m$  as the fraction of the volume  $V_m$  of the  $m$ th shell (core) to the volume  $V_o$  of the nano-ion, expressed as

$$t_m = V_m/V_o = (a_m b_m c_m - a_{m+1} b_{m+1} c_{m+1})/abc \quad (m = 1, 2, \dots, n-1), \quad (2.42a)$$

$$t_n = V_n/V_o = a_n b_n c_n/abc \quad (m = n). \quad (2.42b)$$

The polarizability  $\tilde{\alpha}$ , for the nano-ion defined by

$$\langle \mathbf{P} \rangle = \tilde{\alpha} \mathbf{F}_0, \quad (2.43)$$

is expressed from Eqs. (2.41) and (2.35) as

$$\tilde{\alpha} = \sum_{m=1}^n \{ t_m (\tilde{\epsilon}_m - \tilde{\epsilon}_0) \tilde{\mathbf{S}}_m \}. \quad (2.44)$$

For a spherical, core/shell structured particle ( $n=2$ ), we confirmed that the polarizability given by Eq. (2.44) reduces to that reported in literature.<sup>41</sup>

### C. Effective dielectric permittivity tensor

Now, we derive the effective dielectric permittivity tensor for the composite containing the ellipsoidal nano-ions dispersed in a host medium at a volume fraction  $f$ . The nano-ions are, as already shown in Fig. 1, the same in shape and orientation (principal axes parallel to  $x$ ,  $y$ , and  $z$  directions) but not necessarily in size. The exciting light field  $\langle \mathbf{E} \rangle$  is not equal to  $\mathbf{F}_0$  but is given by averaging the uniform, quasistatic fields  $\mathbf{F}_m$ 's over the matrix and the core and shells of the nano-ions as

$$\langle \mathbf{E} \rangle = (1-f) \mathbf{F}_0 + f \sum_{m=1}^n t_m \mathbf{F}_m. \quad (2.45)$$

Substituting Eq. (2.35) into Eq. (2.45), we obtain

$$\langle \mathbf{E} \rangle = \left\{ (1-f) \tilde{\mathbf{I}} + f \sum_{m=1}^n t_m \tilde{\mathbf{S}}_m \right\} \mathbf{F}_0. \quad (2.46)$$

The total electric flux density  $\langle \mathbf{D} \rangle$  for the whole composite relative to the matrix with the permittivity tensor  $\tilde{\epsilon}_0$  is expressed as

$$\langle \mathbf{D} \rangle = \tilde{\epsilon}_0 \langle \mathbf{E} \rangle + f \langle \mathbf{P} \rangle. \quad (2.47)$$

Therefore, the effective permittivity tensor  $\langle \tilde{\epsilon} \rangle$  for the composite defined by

$$\langle \mathbf{D} \rangle = \langle \tilde{\epsilon} \rangle \langle \mathbf{E} \rangle \quad (2.48)$$

is finally obtained by substituting Eqs. (2.43), (2.44), and (2.46) into Eq. (2.47) to the form

$$\langle \tilde{\epsilon} \rangle = \tilde{\epsilon}_0 + f \left\{ \sum_{m=1}^n t_m (\tilde{\epsilon}_m - \tilde{\epsilon}_0) \tilde{\mathbf{S}}_m \right\} \left\{ (1-f) \tilde{\mathbf{I}} + f \sum_{m=1}^n t_m \tilde{\mathbf{S}}_m \right\}^{-1}. \quad (2.49)$$

We can simplify Eq. (2.49) to

$$\langle \tilde{\epsilon} \rangle = \tilde{\epsilon}_0 + f \left\{ \sum_{m=1}^n t_m (\tilde{\epsilon}_m - \tilde{\epsilon}_0) \langle \tilde{\mathbf{S}}_m \rangle \right\}, \quad (2.50)$$

by defining

$$\langle \tilde{\mathbf{S}}_m \rangle = \tilde{\mathbf{S}}_m \left\{ (1-f) \tilde{\mathbf{I}} + f \sum_{m=1}^n t_m \tilde{\mathbf{S}}_m \right\}^{-1}. \quad (2.51)$$

Combining Eq. (2.35) and Eq. (2.46), we observe that  $\langle \tilde{\mathbf{S}}_m \rangle$  connects  $\mathbf{F}_m$  to the light field  $\langle \mathbf{E} \rangle$  by

$$\mathbf{F}_m = \langle \tilde{\mathbf{S}}_m \rangle \langle \mathbf{E} \rangle. \quad (2.52)$$

We can further rewrite Eq. (2.50) to a brief form as

$$\langle \tilde{\epsilon} \rangle = \sum_{m=0}^n \tilde{\epsilon}_m \Delta_m, \quad (2.53)$$

where  $\Delta_m$ 's ( $m=1-n$ ) are the "virtual" volume fractions for shells and core that are defined as

$$\Delta_m = f t_m \langle \tilde{\mathbf{S}}_m \rangle \quad (m=1, 2, \dots, n), \quad (2.54a)$$

and  $\Delta_0$  is the "virtual" volume fraction for the matrix given by

$$\Delta_0 = 1 - \sum_{m=1}^n \Delta_m. \quad (2.54b)$$

Now let us extend  $\langle \tilde{\epsilon} \rangle$  to the composites containing  $N$  types of nano-onions that differ in shape and/or dielectric constants. Describing the filling factor of the  $j$ th type ( $j=1, 2, \dots, N$ ) of nano-onion ensemble as  $f^j$ , the polarizability is extended from Eq. (2.44) to the following:

$$\tilde{\alpha} = \sum_{j=1}^N \left\{ f^j \sum_{m=1}^{n^j} t_m^j (\tilde{\epsilon}_m^j - \tilde{\epsilon}_0) \tilde{\mathbf{S}}_m^j \right\}. \quad (2.55)$$

Here  $t_m^j$  and  $\tilde{\mathbf{S}}_m^j$  are the volume fraction and field connecting tensor, respectively, for the  $m$ th shell (or core) belonging to the  $j$ th type nano-onions that have  $n^j$ -fold core/shell structure. Equation (2.49) is then extended to

$$\begin{aligned} \langle \tilde{\epsilon} \rangle = & \tilde{\epsilon}_0 + \left[ \sum_{j=1}^N \left\{ f^j \sum_{m=1}^{n^j} t_m^j (\tilde{\epsilon}_m^j - \tilde{\epsilon}_0) \tilde{\mathbf{S}}_m^j \right\} \right] \\ & \times \left[ \left( 1 - \sum_{j=1}^N f^j \right) \tilde{\mathbf{I}} + \sum_{j=1}^N f_j \left\{ \sum_{m=1}^{n^j} t_m^j (\tilde{\epsilon}_m^j - \tilde{\epsilon}_0) \tilde{\mathbf{S}}_m^j \right\} \right]^{-1}. \end{aligned} \quad (2.56)$$

Equation (2.56) is simplified to the form

$$\langle \tilde{\epsilon} \rangle = \tilde{\epsilon}_0 + \sum_{j=1}^N \left\{ f^j \sum_{m=1}^{n^j} t_m^j (\tilde{\epsilon}_m^j - \tilde{\epsilon}_0) \langle \tilde{\mathbf{S}}_m^j \rangle \right\}, \quad (2.57)$$

as we set

$$\langle \tilde{\mathbf{S}}_m^j \rangle = \tilde{\mathbf{S}}_m^j \left[ \left( 1 - \sum_{j=1}^N f^j \right) \tilde{\mathbf{I}} + \sum_{j=1}^N f_j \left\{ \sum_{m=1}^{n^j} t_m^j (\tilde{\epsilon}_m^j - \tilde{\epsilon}_0) \tilde{\mathbf{S}}_m^j \right\} \right]^{-1}. \quad (2.58)$$

### III. RESONANCE CONDITIONS AND SURFACE PLASMON EIGENMODES

In this section, we derive the conditions in which dipolar surface plasmon resonance occurs in the composites containing the  $n$ -fold nano-onions, and investigate the symmetry of the plasmon eigenmodes from the polarity of the charges induced on the metal surfaces. The metal in the nano-onions is assumed to have dielectric function  $\epsilon(\omega)$  ( $\omega$ : light angular frequency) of Drude type due to free electron gas as follows:<sup>31</sup>

$$\epsilon(\omega) = \epsilon'(\omega) + i\epsilon''(\omega) = 1 - \frac{\omega_p^2}{\omega^2 + \gamma^2} + i \frac{\gamma \omega_p^2}{\omega(\omega^2 + \gamma^2)}. \quad (3.1)$$

Here  $\omega_p$  is the volume plasmon angular frequency and  $\gamma$  the relaxation constant that is responsible for the dielectric loss or the imaginary dielectric function,  $\epsilon''(\omega)$ , of the metal. The real dielectric function  $\epsilon'(\omega)$  becomes zero at  $\omega' = \sqrt{\omega_p^2 - \gamma^2}$ , where in bulk metal samples volume charge density waves are resonantly excited. In the range  $\omega < \omega'$ ,  $\epsilon'(\omega)$  becomes negative in sign, which facilitates the excitation of the surface charge density waves or the surface plasmon resonance.

Let us consider an unstructured ( $n=1$ ) metal particle ellipsoidal in shape. When a quasistatic electric field  $F_0^x$  is applied to the particle along the  $x$  direction by the deriving light wave, a uniform electric field  $F_1^x$  is induced parallel to the light field inside the particle. The field is obtained by substituting Eqs. (2.31a) and (2.37) into Eq. (2.35) as

$$F_1^x = \frac{F_0^x}{1/(\tilde{\mathbf{S}}_1)_{xx}} = \frac{1}{(\tilde{\mathbf{A}}_1)_{xx}} F_0^x, \quad (3.2a)$$

$$(\tilde{\mathbf{A}}_1)_{xx} = \frac{N_1^x \epsilon_1 + (1 - N_1^x) \epsilon_0}{\epsilon_0}. \quad (3.2b)$$

Therefore, when

$$\text{Re}[1/(\tilde{\mathbf{S}}_1)_{xx}] = 0, \quad (3.3a)$$

or

$$\text{Re}[(\tilde{\mathbf{A}}_1)_{xx}] = 0, \quad (3.3b)$$

and, thus

$$\text{Re}[\epsilon_1] = -\frac{1 - N_1^x}{N_1^x} \quad (3.4)$$

holds, the induced field  $F_1^x$  takes the resonant maximum value given by<sup>35</sup>

$$F_1^x = -i \frac{1}{\text{Im}[1/(\tilde{\mathbf{S}}_1)_{xx}]} F_0^x = -i \frac{1}{\text{Im}[(\tilde{\mathbf{A}}_1)_{xx}]} F_0^x. \quad (3.5)$$

Because this field is 90° out of phase with the driving optical field ( $F_0^x$ ), the particles absorb maximum light power at the resonance frequency, similar to a resonantly driven cavity.<sup>46</sup> The quality factor  $Q$  of the resonance is inversely proportional to  $\text{Im}[1/(\tilde{\mathbf{S}}_1)_{xx}]$ .<sup>35</sup> If the metal has no dielectric loss ( $\gamma=0$ ), or  $\text{Im}[\epsilon_1]=0$  and thus  $\text{Im}[1/(\tilde{\mathbf{S}}_1)_{xx}]=0$ ,  $F_1^x$  and  $Q$  become infinitely large. Therefore, even if the external field ( $F_0^x$ ) is absent, the inner field ( $F_1^x$ ) oscillating at the resonance frequency can exist, which induces inside the particle the polarization and excites the charge density waves on the particle surface. This is the surface plasma resonance in an ellipsoidal metal particle.

For the composite containing the  $n$ -fold nano-onions, the condition in which surface plasmon resonance occurs in the  $m$ th shell (or core) is given by extending Eq. (3.3a) to

$$\text{Re}[1/\langle\tilde{\mathbf{S}}_m\rangle_{xx}] = 0 \quad (m = 1, 2, \dots, n). \quad (3.6)$$

Here  $\langle\tilde{\mathbf{S}}_m\rangle$  connects the light field  $\langle\mathbf{E}\rangle$  to the internal field  $\mathbf{F}_m$  as in Eq. (2.52). When resonated, the  $m$ th shell absorbs maximum light power, which is analogous to the dissipative  $m$ -fold coupled oscillators with dampers.<sup>45</sup> By substituting Eq. (2.36) into Eq. (3.6), we can rewrite the resonance condition as follows:

$$\text{Re}\{[\tilde{\mathbf{T}}_1][\tilde{\mathbf{T}}_2] \cdots [\tilde{\mathbf{T}}_n]_{1,1} \{[\tilde{\mathbf{T}}_{m+1}][\tilde{\mathbf{T}}_{m+2}] \cdots [\tilde{\mathbf{T}}_n]_{1,1}^{-1}\}_{xx}\} = 0. \quad (3.7)$$

If the nano-onions and the surrounding medium are nonmagnetic (i.e.,  $\varepsilon_m^{xy} = \varepsilon_m^{yz} = \varepsilon_m^{zx} = 0$ ;  $m = 0, 1, \dots, n$ ) having no dielectric losses (i.e.,  $\text{Im}[\tilde{\varepsilon}_m] = 0$ ;  $m = 0, 1, \dots, n$ ), all the components of the super matrices  $\tilde{\mathbf{T}}_m$  given in Eq. (2.31) become diagonal tensors with real number components. Equation (3.7) then reduces to the form

$$\{[\tilde{\mathbf{T}}_1][\tilde{\mathbf{T}}_2] \cdots [\tilde{\mathbf{T}}_n]_{1,1}\}_{xx} \{[\tilde{\mathbf{T}}_{m+1}][\tilde{\mathbf{T}}_{m+2}] \cdots [\tilde{\mathbf{T}}_n]_{1,1}^{-1}\}_{xx} = 0, \quad (3.8)$$

because both  $\{[\tilde{\mathbf{T}}_1][\tilde{\mathbf{T}}_2] \cdots [\tilde{\mathbf{T}}_n]_{1,1}\}$  and  $\{[\tilde{\mathbf{T}}_{m+1}] \times [\tilde{\mathbf{T}}_{m+2}] \cdots [\tilde{\mathbf{T}}_n]_{1,1}^{-1}\}$  are also diagonal tensors. From Eq. (3.8) we have  $n$  resonance angular frequencies,  $\omega_1, \omega_2, \dots, \omega_n$ , which are the solutions for the  $n$ th order equation of  $\omega$ :

$$\{[\tilde{\mathbf{T}}_1][\tilde{\mathbf{T}}_2] \cdots [\tilde{\mathbf{T}}_n]_{1,1}\}_{xx} = 0. \quad (3.9)$$

We also have  $n-m$  anti-resonance frequencies, where zero field is induced in the  $m$ th shell or core,<sup>46</sup> obtained by solving the  $(n \text{ minus } m)$ -th order equation of  $\omega$

$$\{[\tilde{\mathbf{T}}_{m+1}][\tilde{\mathbf{T}}_{m+2}] \cdots [\tilde{\mathbf{T}}_n]_{1,1}\}_{xx} = 0. \quad (3.10)$$

When Eq. (3.10) holds,  $1/\langle\tilde{\mathbf{S}}_m\rangle_{xx}$  ( $\propto\{[\tilde{\mathbf{T}}_{m+1}] \times [\tilde{\mathbf{T}}_{m+2}] \cdots [\tilde{\mathbf{T}}_n]_{1,1}^{-1}\}_{xx}$ ) diverges to infinities, and thus Eq. (2.52) yields  $\mathbf{F}_m = 0$ .

The charge density  $\sigma_m$  induced on the  $m$ th boundary surface by the light field  $\langle\mathbf{E}^x\rangle$  is formulated from Eqs. (2.40) and (2.52) as follows:

$$\sigma_m^x = P_m^x - P_{m-1}^x = \{(\varepsilon_m - \varepsilon_0)\langle\tilde{\mathbf{S}}_m\rangle_{xx} - (\varepsilon_{m-1} - \varepsilon_0)\langle\tilde{\mathbf{S}}_{m-1}\rangle_{xx}\} \times \langle\mathbf{E}^x\rangle \quad (m = 1, 2, 3, \dots, n). \quad (3.11)$$

If no dielectric loss exists in the shells (or core), and thus no phase retardance exists between the outer and inner surfaces of a metal shell, we can determine by  $\sigma_m^x/\sigma_{m-1}^x$  whether the surface plasmon polariton eigenmodes excited in the  $m$ th shell are symmetric or anti-symmetric.

#### IV. SURFACE PLASMONS IN COMPOSITE CONTAINING Na/DIELECTRIC NANO-ONIONS

##### A. Resonant light extinction and symmetry of plasmon eigenmodes

First, we consider nonmagnetic nano-onions of spherical shape for simplicity, having

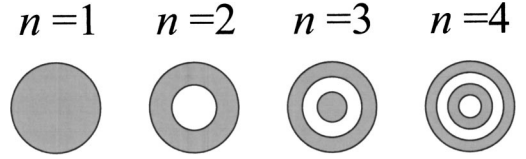


FIG. 3. Spherical nano-onions of alternate Na (shaded area) and dielectric shells and core.

$$N_m^x = N_m^y = N_m^z = 1/3, \quad (4.1a)$$

$$a_m = b_m = c_m \quad (m = 1, 2, 3, \dots, n). \quad (4.1b)$$

Starting from a Na sphere ( $n=1$ ), an inner core of a dielectric and that of Na are added by turns, as shown in Fig. 3. Here we assume

$$a_1 - a_2 = a_2 - a_3 = \cdots = a_{n-1} - a_n = a_n, \quad (4.2)$$

or the core radius is equal to each shell thickness. We also assume that Na has  $\hbar\omega_p = 5.95$  eV and  $\hbar\gamma = 0.31$  eV as reported in literature,<sup>3</sup> and the dielectric has  $\varepsilon = 10$  independent of photon energy, similar as assumed by Sinzig and Quinten.<sup>39</sup> Such a fictitious, high permittivity was chosen for better recognition of the effect of adding the dielectric to the metal. The nano-onions are dispersed in a matrix with  $\varepsilon_0 = 1$  (as in vacuum, similar as Sinzig and Quinten<sup>39</sup>) at a volume fraction of  $f = 0.01$ . We assumed such a small filling factor to conform to MG theory and to reduce the imaginary (or loss) term of  $\langle\tilde{\mathbf{S}}_m\rangle_{xx}$ , thus facilitating the resonance even at low photon energy range, where  $\hbar\gamma$  approaches  $\hbar\omega$ .

For the composites containing the nano-onions with stacking number  $n=1-7$ , we calculated the light extinction coefficient

$$\kappa = \text{Im}[\langle\tilde{\varepsilon}\rangle_{xx}]^{1/2} \quad (4.3)$$

as a function of  $\hbar\omega$  in the range 0.4–6 eV. Figure 4 shows semi-logarithmic plots of  $\kappa$ , in which the spectra are shifted along the ordinate by arbitrary factors for better presentation. The  $n$ -fold nano-onions exhibit  $n$  resonant absorption peaks at  $\hbar\omega = \hbar\omega_1, \hbar\omega_2, \dots, \hbar\omega_n$ , except  $n=7$ , where the lowest resonant energy  $\hbar\omega_7$  runs off the lower limit of the calcula-

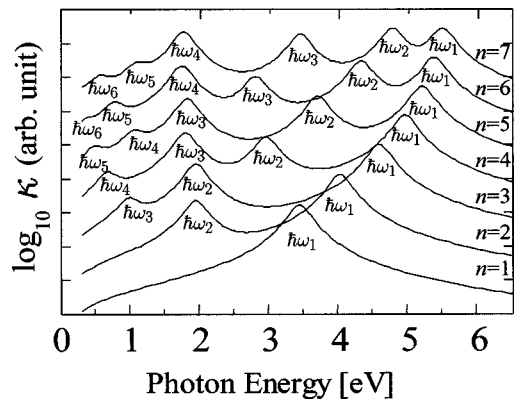


FIG. 4. Extinction coefficient spectra (shifted along the ordinate by arbitrary factors) calculated for composites containing spherical,  $n$ -fold Na/dielectric nano-onions at a volume fraction of  $f = 0.01$ .

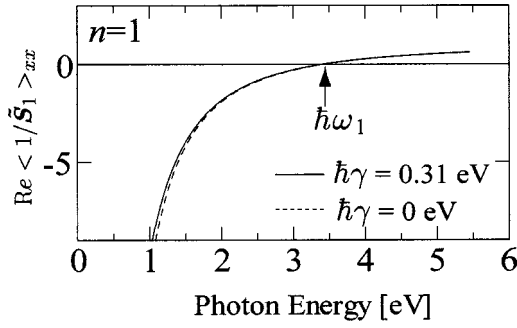


FIG. 5.  $\text{Re}[1/\langle\tilde{S}_1\rangle_{xx}]$  calculated as a function of photon energy for a composite which contains spherical, nonstructured nanoparticles of Na having  $\hbar\gamma$  as reported in the literature (shown by solid line) and  $\hbar\gamma=0$  (dotted line).

tion range. The peak-position frequencies are very close to the surface plasmon resonance frequencies, where  $\text{Re}[1/\langle\tilde{S}_m\rangle_{xx}]=0$  holds, as shown in Figs. 5–7 for  $n=1, 2$ , and 4, respectively. This is similar as in the forced harmonic motion of the dissipative, coupled oscillators.<sup>45</sup>

In Figs. 5–7 we compare the spectra of  $\text{Re}[1/\langle\tilde{S}_m\rangle_{xx}]$  with those calculated assuming  $\hbar\gamma=0$  in order to investigate the effect of the dielectric loss. For the simple Na spheres ( $n=1$ ) the resonance occurs at  $\hbar\omega_1=3.4$  eV (Fig. 5), which does not change appreciably by introducing the dielectric loss. Figure 6 shows that as the dielectric core is inserted at the center of the Na sphere, thus making  $n=2$ , the resonance energy  $\hbar\omega_1$  shifts to higher values, and another resonance appears at a lower energy  $\hbar\omega_2$ . When  $\hbar\gamma=0$  [Fig. 6(a)'],  $\text{Re}[1/\langle\tilde{S}_1\rangle_{xx}]$  diverges to infinity at an anti-resonance energy  $\hbar\omega_a$  between  $\hbar\omega_1$  and  $\hbar\omega_2$ . When  $\hbar\gamma\neq 0$  [Fig. 6(a)], the diverging curve of  $[1/\langle\tilde{S}_1\rangle_{xx}]$  is deformed to a continuous curve crossing the horizontal axis at  $\hbar\omega_a$ .

Figures 5–7 indicate that when  $\hbar\gamma=0$ , each  $n$ -fold nano-onion has  $n$  eigenfrequencies ( $\omega_1, \omega_2, \dots, \omega_n$ ), and each  $m$ th shell (or core) has  $n-m$  anti-resonance frequencies ( $\omega_a, \omega_b, \omega'_a$ , etc.), as is expected from Eqs. (3.9) and (3.10). Introducing the dielectric loss smears out some of the resonance and the anti-resonance [e.g.,  $\hbar\omega_4$  and  $\hbar\omega_c$  in Figs. 7(a) and 7(a)', respectively].

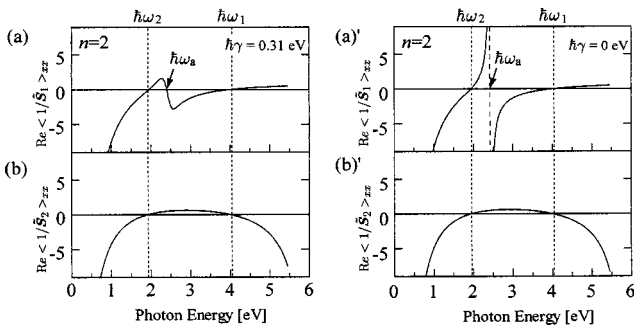


FIG. 6.  $\text{Re}[1/\langle\tilde{S}_1\rangle_{xx}]$  and  $\text{Re}[1/\langle\tilde{S}_2\rangle_{xx}]$  calculated for a composite which contains spherical, twofold ( $n=2$ ) core (dielectric)/shell (Na) structured nano-onions, using  $\hbar\gamma$  as reported in the literature [(a) and (b)] and  $\hbar\gamma=0$  [(a)' and (b)'].

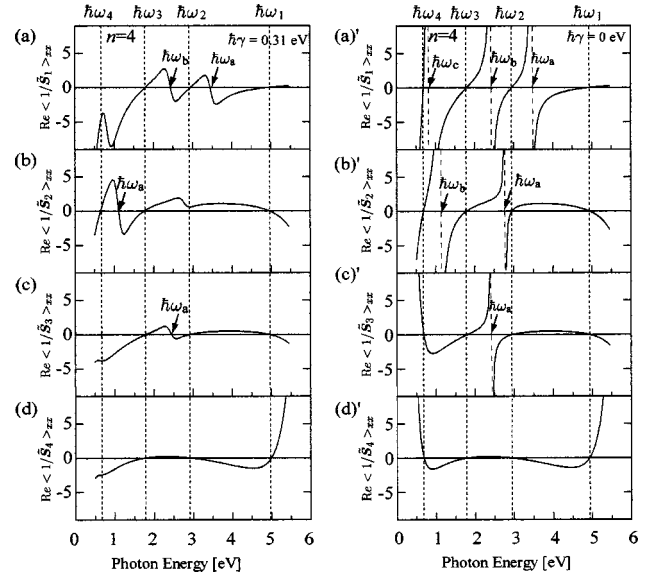


FIG. 7.  $\text{Re}[1/\langle\tilde{S}_m\rangle_{xx}]$  ( $m=1-4$ ) calculated for a composite which contains spherical, fourfold ( $n=4$ ) nano-onions, using  $\hbar\gamma$  as reported in the literature [(a)–(d)] and  $\hbar\gamma=0$  [(a)'–(d)'].

Assuming  $\hbar\gamma=0$ , we calculated from Eq. (3.11) surface charge densities induced on the  $m$ th surface, with which we determined their polarity and thus the symmetry of the surface plasmon eigenmodes induced in the Na shells, as given in Table I. Letters S and A in the table indicate symmetric and anti-symmetric eigenmodes (cf. Fig. 8),<sup>25,39</sup> respectively. For example, when  $n=4$  (i.e., fourfold nano-onions) at  $\hbar\omega_1$ , charge densities  $+, +, -, +$  in sign are induced on the surfaces of numbers  $m=1, 2, 3$ , and 4, respectively. Thus, the Na shell has symmetric and anti-symmetric surface plasmon modes on its outer ( $m=1$  and 2) and inner ( $m=3$  and 4) shells, respectively. One will notice that in all nano-onions with  $n=2-5$ , the outermost ( $m=1$  and 2) Na shell has only symmetric eigenmodes at  $\hbar\omega_1$ , while it has only anti-symmetric eigenmodes at other resonance energies,  $\hbar\omega_2, \hbar\omega_3, \hbar\omega_4$ , and  $\hbar\omega_5$ .

## B. Magneto-optical enhancement

Applying an external magnetic field of  $B=1$  T along the  $z$  axis, we calculate the magneto-optical Kerr effect for the composite containing the spherical nano-onions. The off-diagonal dielectric function  $\epsilon_m^{xy} = \epsilon_m^{xy'} + i\epsilon_m^{xy''}$  for Na is expressed in terms of the cyclotron angular frequency  $\omega_c$ , as well as  $\omega_p$  and  $\gamma$  for the free electrons as follows:<sup>46</sup>

$$\epsilon_m^{xy} = -\epsilon_m^{yx} = i\omega_c \frac{\omega_p^2}{\omega(\omega + i\gamma)^2 - \omega_c^2}, \quad (4.4a)$$

$$\omega_c = eB/m^*. \quad (4.4b)$$

Here,  $e$  and  $m^*$  are charge and effective mass of the electrons, respectively. The polar Kerr rotation angle  $\theta_K$  and ellipticity angle  $\chi_K$  for the composite containing the nano-onions were calculated from the complex equation

TABLE I. Polarity of surface charge densities induced on the  $m$ th surfaces and symmetry (S: symmetric, A: anti-symmetric) of surface plasmon eigenmodes generated in the Na shells in spherical,  $n$ -fold Na/dielectric nano-onions, calculated at respective resonance energies. Parentheses indicate that the resonance is smeared as  $\hbar\gamma$  is changed from 0 to 0.31 eV, the literature value.

Resonance energy	Surface number $m$	$n=5$		$n=4$		$n=3$		$n=2$		$n=1$
		Polarity	Symmetric	Polarity	Symmetric	Polarity	Symmetric	Polarity	Symmetric	Polarity
$\hbar\omega_1$	1	+	S	+	S	+	S	+	S	+
	2	+		+		+		+		
	3	-	S	-	A	-	A	-	A	-
	4	-		+		+		+		
	5	(+)								
$\hbar\omega_2$	1	+	A	+	A	+	A	+	A	
	2	(-)		(-)		(-)		(-)		
	3	+	S	+	S	+	S	+	S	
	4	+		+		+		+		
	5	(-)								
$\hbar\omega_3$	1	+	A	+	A	(+)	A		A	
	2	-		-		-		-		
	3	+	A	(+)	A	-	A		A	
	4	-		-		-		-		
	5	(+)								
$\hbar\omega_4$	1	(+)	A	(-)	A		A		A	
	2	(-)		(+)		(+)		(+)		
	3	(+)	A	(-)	A		A		A	
	4	(-)		(+)		(+)		(+)		
	5	-								
$\hbar\omega_5$	1	(+)	A		A		A		A	
	2	-								
	3	(-)	A		A		A		A	
	4	(+)								
	5	(+)								

$$\theta_K + i\chi_K = \frac{i\langle \tilde{\epsilon} \rangle_{xy}}{\sqrt{\langle \tilde{\epsilon} \rangle_{xx}(\langle \tilde{\epsilon} \rangle_{xx} - 1)}}. \quad (4.5)$$

As an example, the case for  $n=2$  is shown in Fig. 9. The diagonal and off-diagonal elements of the complex effective dielectric tensor,  $\langle \tilde{\epsilon} \rangle_{xx} (= \langle \tilde{\epsilon}' \rangle_{xx} + i\langle \tilde{\epsilon}'' \rangle_{xx})$  and  $\langle \tilde{\epsilon} \rangle_{xy} (= \langle \tilde{\epsilon}' \rangle_{xy} + i\langle \tilde{\epsilon}'' \rangle_{xy})$ ,

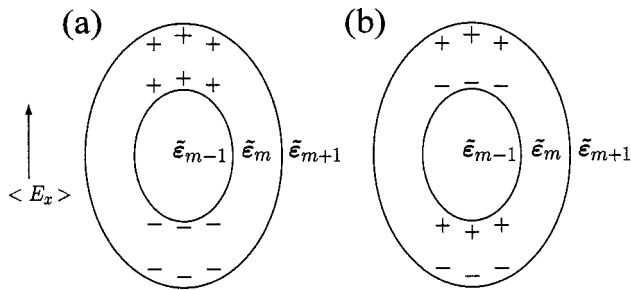


FIG. 8. Surface charges induced in the  $m$ th shell by (a) symmetric and (b) antisymmetric surface plasmon eigenmodes.

exhibit resonant dispersion relations in close vicinity of the surface plasmon resonance frequencies as shown in Fig. 9. However, the Kerr rotation  $\theta_K$  and ellipticity  $\chi_K$  exhibit a resonant dispersion relation at frequencies slightly different from the surface plasmon resonance frequencies. This is because at these frequencies  $\langle \tilde{\epsilon} \rangle_{xx} - 1$ , which appears in the denominator on the right side of Eq. (4.5), approaches zero.

Figure 10 shows  $\theta_K$  and  $\chi_K$  for  $n=3$ . Because Na fills the composite by factor  $f(t_1+t_3)$ , we defined Kerr effect enhancement factors by

$$M(\theta_K) = \frac{\theta_K^p(\text{comp})}{f(t_1+t_3)\theta_K(\text{Na})}, \quad (4.6a)$$

$$M(\chi_K) = \frac{\chi_K^p(\text{comp})}{f(t_1+t_3)\chi_K(\text{Na})}. \quad (4.6b)$$

Here,  $\theta_K^p(\text{comp})$  [or  $\chi_K^p(\text{comp})$ ] expresses the resonant peak height of the Kerr rotation (ellipticity) for the composite and

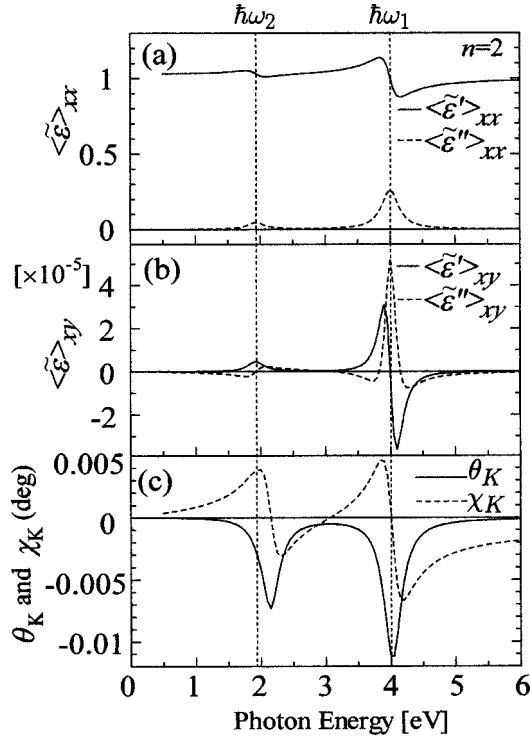


FIG. 9. Spectra for effective dielectric permittivity tensor elements and Kerr effect calculated for a composite containing spherical, twofold Na/dielectric nano-ions.

$\theta_K(\text{Na})$  [ $\chi_K(\text{Na})$ ] expresses the rotation (ellipticity) calculated for Na bulk sample at resonance frequencies. As shown in Table II, we obtained for  $n=3$ ,  $M(\theta_K)$  and  $M(\chi_K) \approx 6-90$ , which increased about one order of magnitude, to  $\approx 80-1700$ , when  $\hbar\gamma$  was hypothetically reduced by a factor 5, from 0.31 to 0.06 eV. Thus, the magneto-optical en-

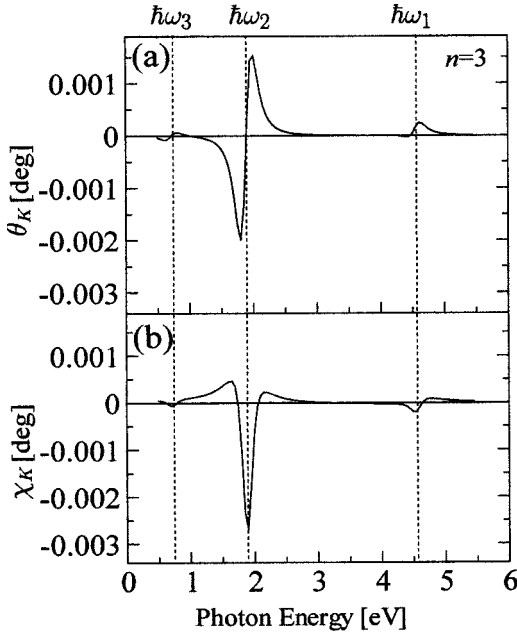


FIG. 10. Kerr effect spectra calculated for a composite containing spherical, threefold Na/dielectric nano-ions.

TABLE II. Enhancement factors for Kerr rotation and ellipticity for a composite containing spherical, threefold ( $n=3$ ) nano-ions calculated at the respective resonance energies for two values of  $\hbar\gamma$ .

	$M(\theta_K)$		$M(\chi_K)$	
	$\hbar\gamma=0.31$ eV <sup>a</sup>	$\hbar\gamma=0.06$ eV <sup>b</sup>	$\hbar\gamma=0.31$ eV <sup>a</sup>	$\hbar\gamma=0.06$ eV <sup>b</sup>
$\hbar\omega_1$	7.7	82	10	82
$\hbar\omega_2$	56	1166	88	1698
$\hbar\omega_3$	6.1	159	6.4	85

<sup>a</sup>Reported in the literature.

<sup>b</sup>Reduced by a factor 5 from the literature value.

hancement factor is augmented as the  $Q$  factor of the resonance becomes high.

### C. Effect of the shape of nano-ions

Next, we changed the shape of the nano-ions to spheroidal prolate ( $N_x=N_y=0.35$ ) and oblate ( $N_x=N_y=0.28$ ) to determine how the depolarization factor affects the magneto-optical response. For the composites containing the spheroidal, twofold ( $n=2$ ) nano-ions we calculated  $\langle \tilde{\epsilon} \rangle_{xy}$  and Kerr effect. The results are shown in Figs. 11 and 12. Comparing Fig. 11 (prolate) with Fig. 9 (spherical), one notices that increasing the depolarization factor  $N_x$  along the light field direction augments the resonant peak heights of  $\langle \tilde{\epsilon} \rangle_{xy}$ ,  $\theta_K$ , and  $\chi_K$  at  $\hbar\omega_1$  slightly, but does not change appreciably the peak heights at  $\omega_2$ . On the other hand, Fig. 12 (oblate) shows that decreasing  $N_x$  deforms the resonant curves and decreases their peak heights of the Kerr effect at both  $\hbar\omega_1$  and  $\hbar\omega_2$ .

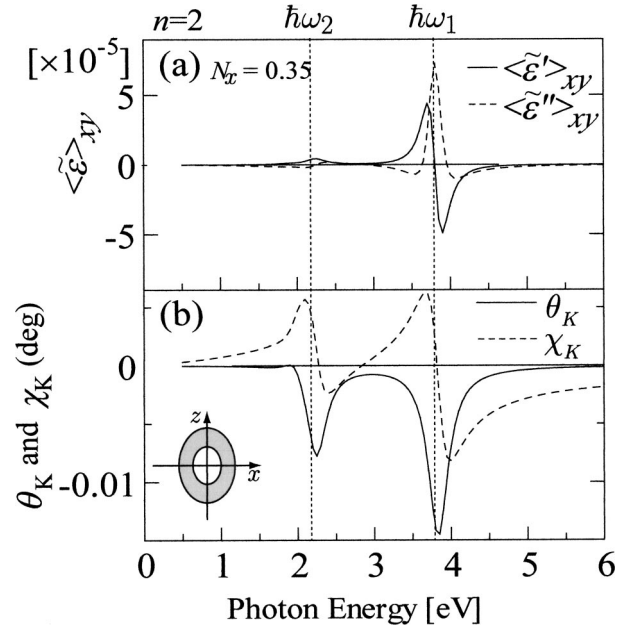


FIG. 11. Off-diagonal element for effective dielectric permittivity tensor and Kerr effect calculated for a composite containing prolate, twofold Na/dielectric nano-ions.

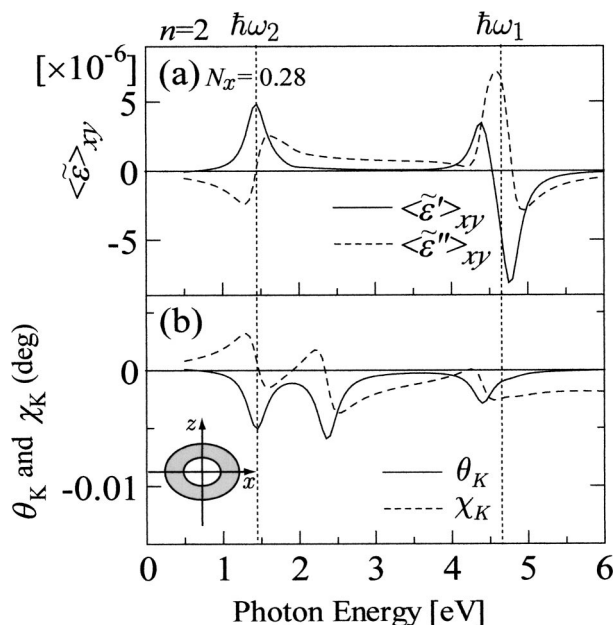


FIG. 12. Off-diagonal element for dielectric permittivity tensor and Kerr effect calculated for a composite containing oblate, two-fold Na/dielectric nano-ions.

## V. DISCUSSION AND CONCLUSION

By applying the MG theory, which is based on the quasistatic approximation, we formulated the effective dielectric permeability tensors for the composites containing ellipsoidal,  $n$ -fold nano-ions as given by Eq. (2.49), or in more simplified forms of Eqs. (2.50) and (2.53). When there are two or more different types of nano-ions dispersed in the matrix, the formula is extended as given by Eq. (2.57). Because the polarizations induced in the nano-ions are treated as point dipole moments in our quasistatic approximation, the size of the nano-ions does not appear in the effective dielectric tensor explicitly, but enters as the filling factors  $f$  and  $t_m$ .

Using the effective dielectric tensor, we analytically formulated the resonance conditions for the dipolar surface plasmons as Eq. (3.6). We also derived Eq. (3.11), a formula giving the surface charge density induced on the shell surfaces, with which we can determine the symmetry of the surface plasmon polariton eigenmodes excited in the metal shells.

On the composites containing model nano-ions spherical in shape having  $n$ -fold Na/dielectric alternate stratification, our findings are summarized as follows.

(1) If the dielectric loss of Na is neglected, there are  $n$  surface plasmon eigenmodes, in each of which an infinitely large electric field is induced in every shell or core. In addition in the  $m$ th shell or core, anti-resonance (where zero field is induced) occurs at  $n-m$  frequencies. The occurrence of the resonance and anti-resonance is similar as found in the  $n$ -fold coupled oscillators.<sup>45</sup>

(2) As the dielectric loss is introduced, the light extinction coefficient exhibits resonant peaks at the surface plasma frequencies, although some of the resonance and anti-

resonance (which occurred in case of no dielectric loss) are smeared out.

(3) The magneto-optical Kerr effect, as well as the off-diagonal dielectric permittivity tensor elements, is prominently enhanced by the surface plasmon resonance, especially when the dielectric loss is weak and the resonance has a high quality factor  $Q$ . For the Na/dielectric double layered nano-ions, we found that changing the particles shape to prolate spheroidal (and thus increasing the depolarization factor) increases the resonant peak heights of  $\langle \tilde{\epsilon} \rangle_{xy}$ ,  $\theta_K$ , and  $\chi_K$  at  $\omega_1$  only slightly.

We<sup>47</sup> have given a preliminary report on the effective permittivity tensor [Eq. (2.49)], with only a brief outline of its derivation, and have calculated the magneto-optical Kerr effect in composites containing nano-ions of Fe/Au multicore-shell structures; they did not show definite features of plasma resonance in Au shells. We<sup>48</sup> later found that inserting a dielectric layer between the Fe core and Au shell, and thus increasing the  $Q$  factor of the resonance, enhances Kerr effect. This is similar as increasing  $Q$  by decreasing  $\hbar\gamma$  in Na enhances Kerr effect in the composite containing Na/dielectric nano-ions.

The composite containing threefold Na/dielectric nano-ions have large Kerr effect enhancement factors [ $M(\theta_K)$  and  $M(\chi_K) \approx 6-90$ ], which are, however, augmented by a factor  $1/f(t_1+t_2)$  ( $=1/135$ ); actual  $\theta_K$  and  $\chi_K$  are reduced by factors of 0.05–0.7 from those for bulk Na. The figures of merit for the Kerr effect, defined by  $R^{1/2}\theta_K$  and  $R^{1/2}\chi_K$  ( $R$ : reflectivity), are reduced more, by factors of 0.01–0.14, because the composite has a much lower reflectivity ( $R \approx 0.04$ ) than Na bulk ( $R \approx 0.9$ ). This, as well as the combustible nature of Na, makes the composites containing the Na/dielectric nano-ions unfeasible for practical applications, although they provide a good model to study optical surface plasmon resonance.

In our calculation, the filling factor of the nano-ions was fixed to  $f=0.01$ , small enough to conform to the MG theory that was derived assuming sparse dispersion of the particles. Let us reexamine the low filling factor limit in the calculations based on the MG theory. The MG theory<sup>26</sup> was derived originally utilizing the Rayleigh scattering theory, a kind of quasistatic approximation, which assumes that homogeneous fields are induced within and outside the particles by the light field. In other words, the MG theory presupposes that the particles are much smaller than the light wavelength and the particles are sparsely filling the matrix. However, the MG theory has been applied beyond the low filling factor limit, and is justified by experimental results. Kreibig *et al.*<sup>49</sup> revealed that the plasmon resonance absorption spectra for the composites containing Ag spherical nanoparticles (8–75 nm in diameter) are fitted by the MG theory rather well even for high filling factor, up to  $f=0.4$ , as long as the particles were not coagulated. When the composites had partial coagulation, additional peaks appeared, which was explained in term the surface plasma resonance in various types of clusters of the Ag nanoparticles. Therefore, the MG theory is shown to be applicable even for high volume fraction of the particles when no coagulation aggregates exist.

One can explain this as follows. The MG theory is considered as a generalization of the Clausius-Mossotti theory<sup>50</sup>

that gives the dielectric constant for crystals, i.e., the ensembles of spherical atoms in vacuum to the ensembles of the small particles in the matrix. In the MG theory, the local field acting on the particles is approximated by the Lorentz local field, similar as in Clausius-Mossotti theory.<sup>31,42,51</sup> The Clausius-Mossotti theory is applicable to cubic crystals or completely disordered amorphous crystals, in which vacuum is embedded with atoms at a fairly large filling factor, even up to  $\sim 0.74$ , the maximum value obtained for bcc or hexagonal close packing of spherical atoms. Therefore, the MG theory will be applicable even up to large value of  $f$ , when the matrix surrounding the particles are composed of grains much smaller than the particles (i.e., the host material can be considered as continuous, similar as vacuum in the Clausius-Mossotti theory) and the particles are uniformly dispersed without being coagulated. If the grains of the surrounding matrix are not sufficiently smaller than the particles, we must use the Bruggeman theory<sup>27</sup> to symmetrize the roles of inclusion (particles) and the host (matrix) when the filling factor is not small.<sup>51</sup> If the particles are coagulated, the effects by clustering of the particles must be taken into account. Therefore, the MG theory will be applicable even when  $f$  is large for an ideal composite in which the nano-onions are dispersed without coagulation in a matrix composed of very small grains.

Now let us discuss the limit inherent in the calculation by the MG theory, comparing with that by the rigorous Mie scattering theory. For Ag spheres with radius  $a$ , the limit allowing 10% difference between the calculations by the MG theory and the Mie theory is estimated as  $a \leq \sim 0.03\lambda$  ( $\lambda$ : light wavelength).<sup>33,35,37</sup> This is about the size perimeter usually taken to delimit the small particle Rayleigh approximation (based on which the MG theory is derived) from the accurate Mie theory, which amount to  $a=6.9$  and  $105$  nm at our measurement boundaries  $\hbar\omega=6$  and  $0.4$  eV, respectively.

As we already described, Sinzig and Quinten<sup>39</sup> revealed using the Mie scattering calculation that the spherical nano-onions (having diameter  $2a=2-12$  nm), which have similar Na/dielectric stratified structure ( $n \leq 7$ ) dispersed in vacuum as ours, exhibit similar plasmon resonant absorption peaks. The background of the extinction spectra ( $\hbar\omega=0.5-6$  eV) rises prominently at higher photon energies, while our extinction spectra (Fig. 4) do not show such a particular increase. This is because the light scattering intensity, calculated by the Mie theory (which involves space dependence of, as well as multipole scattering by, the polarization and field induced in particles), increases as  $a/\lambda$  increases at higher photon energies.<sup>33</sup> However, it should be noted that by the Mie theory the light extinction is calculated from the scattering cross section by a single particle, without considering any mutual interactions between the particles. The Mie calculation is hence limited to the very sparse dispersion of the nano-onions. On the other hand, our calculation is applicable to more concentrated dispersion of the particles, because the MG theory incorporates the interparticle interaction through the local Lorentz field acting on the particles.

It should be also noted that the dielectric function reported for bulk metal samples may not be directly applicable to small particles. If the dimension  $d$  (core radius and shell thickness) for core/shell structured particles becomes compa-

table to the mean free path  $\ell$  of the free electrons, the relaxation constant  $\gamma$  for the metal core or shell(s) is modified from the bulk value  $\gamma_\infty$  to<sup>21,22,29</sup>

$$\gamma = \gamma_\infty(1 + \ell/d). \quad (5.1)$$

Here, the term  $\ell/d$  expresses the effects of free electron collision at the surface. For Na  $\ell$  is reported to be  $34$  nm.<sup>31</sup> Furthermore, for small particles we must consider the quantum size effect and defects, which will also change the dielectric function of the particles.

In conclusion, we have clarified the physical picture of the surface plasma resonance occurring in the  $n$ -fold stratified Na/dielectric nano-onions, and revealed that magneto-optical effect, as well as light extinction, is prominently enhanced by the surface plasmon resonance in the Na shells and cores. Our calculation, based on the MG theory, should prove useful for the composites containing nano-onions even at a high volume fraction as far as the particles much smaller than the light wavelength are dispersed without coagulation and the dielectric functions of the cores and shells of the nano-onions are known.

#### ACKNOWLEDGMENTS

The authors are indebted to Mr. J. Kuroda for his help in developing the computer program and performing the calculations. They are thankful to Prof. Vince Harris of Northeastern University for the critical reading of the manuscript.

#### APPENDIX: DERIVATION OF EQS. (2.21) AND (2.22)

Substituting Eq. (2.14) into Eq. (2.18), we obtain the electric field on the  $m$ th boundary surface as follows:

$$(E_m^\xi)_{\xi_m} = \sum_i h_1^{-1} \left( E_m^i \frac{\partial u^i}{\partial \xi} + \frac{\partial E_m^i}{\partial \xi} u^i \right)_{\xi_m} = \sum_i (\bar{E}_m^i)_{\xi_m} (n_{\xi^i})_{\xi_m}, \quad (A1a)$$

$$(E_m^\eta)_{\xi_m} = \sum_i \left( h_2^{-1} E_m^i \frac{\partial u^i}{\partial \eta} \right)_{\xi_m} = \sum_i (E_m^i)_{\xi_m} (n_{\eta^i})_{\xi_m}, \quad (A1b)$$

$$(E_m^\zeta)_{\xi_m} = \sum_i \left( h_3^{-1} E_m^i \frac{\partial u^i}{\partial \zeta} \right)_{\xi_m} = \sum_i (E_m^i)_{\xi_m} (n_{\zeta^i})_{\xi_m}. \quad (A1c)$$

Here  $(\dots)_{\xi_m}$  indicates  $\xi = \xi_m$ , and we defined

$$\bar{E}_m^i = F_m^i + \beta_m(N_m^i - 1)C_m^i \quad (i = x, y, z), \quad (A2)$$

with  $\beta_m$ ,  $\tilde{\mathbf{N}}_m$ ,  $\tilde{\mathbf{I}}$  given by Eqs. (2.24)–(2.27). We also introduced unitary vectors along the  $\xi$ ,  $\eta$ , and  $\zeta$  coordinates as follows:<sup>44</sup>

$$\mathbf{n}_\xi = (n_{\xi x}, n_{\xi y}, n_{\xi z}) = \left( \frac{1}{h_1} \frac{\partial x}{\partial \xi}, \frac{1}{h_1} \frac{\partial y}{\partial \xi}, \frac{1}{h_1} \frac{\partial z}{\partial \xi} \right), \quad (\text{A3a})$$

$$\mathbf{n}_\eta = (n_{\eta x}, n_{\eta y}, n_{\eta z}) = \left( \frac{1}{h_2} \frac{\partial x}{\partial \eta}, \frac{1}{h_2} \frac{\partial y}{\partial \eta}, \frac{1}{h_2} \frac{\partial z}{\partial \eta} \right), \quad (\text{A3b})$$

$$\mathbf{n}_\zeta = (n_{\zeta x}, n_{\zeta y}, n_{\zeta z}) = \left( \frac{1}{h_3} \frac{\partial x}{\partial \zeta}, \frac{1}{h_3} \frac{\partial y}{\partial \zeta}, \frac{1}{h_3} \frac{\partial z}{\partial \zeta} \right). \quad (\text{A3c})$$

They satisfy the orthonormal relations

$$\mathbf{n}_\xi \cdot \mathbf{n}_\xi = 1, \quad (\text{A4a})$$

$$\mathbf{n}_\xi \cdot \mathbf{n}_\eta = 0, \quad (\text{A4b})$$

$$\mathbf{n}_\xi \times \mathbf{n}_\eta = \mathbf{n}_\zeta, \quad (\text{A4c})$$

$$\mathbf{n}_\xi \times \mathbf{n}_\zeta = -\mathbf{n}_\eta, \quad (\text{A4d})$$

$$\mathbf{n}_\zeta \times \mathbf{n}_\eta = -\mathbf{n}_\xi. \quad (\text{A4e})$$

In deriving Eq. (A1), we used, in addition to Eq. (A4), the relations

$$\left( \frac{\partial A^x}{\partial \xi} \right)_{\xi_m} = \frac{-1}{a_m^3 b_m c_m}, \quad \left( \frac{\partial A^y}{\partial \xi} \right)_{\xi_m} = \frac{-1}{a_m b_m^3 c_m},$$

$$\left( \frac{\partial A^z}{\partial \xi} \right)_{\xi_m} = \frac{-1}{a_m b_m c_m^3}, \quad (\text{A5a})$$

$$(x)_{\xi_m} = 2a_m \left( \frac{\partial x}{\partial \xi} \right), \quad (y)_{\xi_m} = 2b_m \left( \frac{\partial y}{\partial \xi} \right), \quad (z)_{\xi_m} = 2c_m \left( \frac{\partial z}{\partial \xi} \right), \quad (\text{A5b})$$

which are derived from Eqs. (2.4), (2.16), and (2.24)–(2.27).

Substituting Eq. (A1b) into the boundary condition of Eq. (2.20a), we obtain

$$\sum_i (E_m^i)_{\xi_m} (n_{\eta i})_{\xi_m} = \sum_i (E_{m-1}^i)_{\xi_m} (n_{\eta i})_{\xi_m}. \quad (\text{A6})$$

Since  $(E_m^i)_{\xi_m}$  and  $(E_{m-1}^i)_{\xi_m}$  are constants but  $(n_{\eta i})_{\xi_m}$  is a function of  $\eta$  and  $\zeta$ , we must have  $(E_m^i)_{\xi_m} = (E_{m-1}^i)_{\xi_m}$  ( $i=x, y, z$ ), or in vector form,

$$(E_m^i)_{\xi_m} = (E_{m-1}^i)_{\xi_m} \quad (m=1, 2, \dots, n), \quad (\text{A7})$$

in order for Eq. (A6) to hold for arbitrary values of  $\eta$  and  $\zeta$ . Substituting Eq. (A1c) into Eq. (2.20b) as well as gives Eq. (A7).

The left side of the remaining boundary condition [Eq. (2.20c)] is expanded as

$$(D_m^\xi)_{\xi_m} = (\varepsilon_m^{\xi\xi} E_m^\xi + \varepsilon_m^{\xi\eta} E_m^\eta + \varepsilon_m^{\xi\zeta} E_m^\zeta)_{\xi_m}. \quad (\text{A8})$$

Here, we obtain  $(\varepsilon_m^{\xi\xi})_{\xi_m}$  by the unitary transformation as follows:

$$(\varepsilon_m^{\xi\xi})_{\xi_m} = \sum_{i,j} \varepsilon_m^{ij} (n_{\xi i} n_{\xi j})_{\xi_m}$$

$$= \varepsilon_m \sum_i (n_{\xi i})_{\xi_m} (n_{\xi i})_{\xi_m}$$

$$+ \sum_{i \neq j} (\varepsilon_m^{ij} + \varepsilon_m^{ji}) (n_{\xi i} n_{\xi j})_{\xi_m} = \varepsilon_m, \quad (\text{A9})$$

by using Eqs. (2.8b) and (A4a). In a similar way we obtain  $(\varepsilon_m^{\xi\eta})_{\xi_m}$  as

$$(\varepsilon_m^{\xi\eta})_{\xi_m} = \sum_{i,j} \varepsilon_m^{ij} (n_{\xi i})_{\xi_m} (n_{\eta j})_{\xi_m}$$

$$= \varepsilon_m \sum_{i,j} (n_{\xi i})_{\xi_m} (n_{\eta i})_{\xi_m} + \sum_{i \neq j} \varepsilon_m^{ij} (n_{\xi i} n_{\eta j} - n_{\xi j} n_{\eta i})_{\xi_m}$$

$$= - \sum_{i \neq j} \varepsilon_m^{ij} (n_{\zeta k(i,j)})_{\xi_m}, \quad (\text{A10})$$

in which we used Eq. (A4b) and introduced the suffix  $k$  ( $i, j$ ) as

$$k(i, j) = \begin{cases} x & (i, j) = (y, z) \\ y & (i, j) = (z, x) \\ z & (i, j) = (x, y) \end{cases}. \quad (\text{A11})$$

Similarly, we obtain

$$(\varepsilon_m^{\xi\zeta})_{\xi_m} = \sum_{i \neq j} \varepsilon_m^{ij} (n_{\eta k(i,j)})_{\xi_m}. \quad (\text{A12})$$

Substituting Eqs. (A1a), (A9), (A10), and (A12) into Eq. (A8), we get

$$(D_m^\xi)_{\xi_m} = \varepsilon_m \sum_i (\bar{E}_m^i)_{\xi_m} (n_{\xi i})_{\xi_m} + \sum_{i \neq j} (E_m^i)_{\xi_m} \varepsilon_m^{ij} (-n_{\zeta k(i,j)} n_{\eta i}$$

$$+ n_{\eta k(i,j)} n_{\xi i})_{\xi_m}$$

$$= \varepsilon_m \sum_i (\bar{E}_m^i)_{\xi_m} (n_{\xi i})_{\xi_m} + \sum_{i \neq j} (E_m^i)_{\xi_m} \varepsilon_m^{ij} (n_{\xi k[i, k(i,j)]})_{\xi_m}, \quad (\text{A13})$$

which is further transformed to

$$-(D_m^\xi)_{\xi_m} = \{ \varepsilon_m (\bar{E}_m^x)_{\xi_m} + \varepsilon_m^{xy} (E_m^y)_{\xi_m} + \varepsilon_m^{xz} (E_m^z)_{\xi_m} \} (n_{\xi x})_{\xi_m}$$

$$+ \{ \varepsilon_m^{yx} (E_m^x)_{\xi_m} + \varepsilon_m (\bar{E}_m^y)_{\xi_m} + \varepsilon_m^{yz} (E_m^z)_{\xi_m} \} (n_{\xi y})_{\xi_m}$$

$$+ \{ \varepsilon_m^{zx} (E_m^x)_{\xi_m} + \varepsilon_m^{zy} (E_m^y)_{\xi_m} + \varepsilon_m (\bar{E}_m^z)_{\xi_m} \} (n_{\xi z})_{\xi_m}. \quad (\text{A14})$$

Replacing the suffix  $m$  with  $m-1$  in Eq. (A14) gives

$$-(D_{m-1}^\xi)_{\xi_m} = \{ \varepsilon_{m-1} (\bar{E}_{m-1}^x)_{\xi_m} + \varepsilon_{m-1}^{xy} (E_{m-1}^y)_{\xi_m} + \varepsilon_{m-1}^{xz} (E_{m-1}^z)_{\xi_m} \}$$

$$\times (n_{\xi x})_{\xi_m} + \{ \varepsilon_{m-1}^{yx} (E_{m-1}^x)_{\xi_m} + \varepsilon_{m-1} (\bar{E}_{m-1}^y)_{\xi_m}$$

$$+ \varepsilon_{m-1}^{yz} (E_{m-1}^z)_{\xi_m} \} (n_{\xi y})_{\xi_m} + \{ \varepsilon_{m-1}^{zx} (E_{m-1}^x)_{\xi_m}$$

$$+ \varepsilon_{m-1}^{zy} (E_{m-1}^y)_{\xi_m} + \varepsilon_{m-1} (\bar{E}_{m-1}^z)_{\xi_m} \} (n_{\xi z})_{\xi_m}. \quad (\text{A15})$$

Substituting Eqs. (A14) and (A15) into Eq. (2.20c), we obtain the following vector formulas:

$$\begin{aligned} & \varepsilon_{m-1}(\bar{\mathbf{E}}_{m-1})_{\xi_m} + (\tilde{\varepsilon}_{m-1} - \varepsilon_{m-1}\tilde{\mathbf{1}})(\mathbf{E}_{m-1})_{\xi_m} \\ &= \varepsilon_m(\bar{\mathbf{E}}_m)_{\xi_m} + (\tilde{\varepsilon}_m - \varepsilon_m\tilde{\mathbf{1}})(\mathbf{E}_m)_{\xi_m} \\ & \quad (m = 1, 2, \dots, n). \end{aligned} \quad (\text{A16})$$

By substituting Eqs. (2.14d) and (A2) into Eqs. (A7) and (A16), we get

$$\mathbf{F}_{m-1} + \beta_m \tilde{\mathbf{N}}_m \mathbf{C}_{m-1} = \mathbf{F}_m + \beta_m \tilde{\mathbf{N}}_m \mathbf{C}_m, \quad (\text{A17})$$

$$\begin{aligned} & \tilde{\varepsilon}_{m-1} \mathbf{F}_{m-1} + \beta_m (\tilde{\varepsilon}_{m-1} \tilde{\mathbf{N}}_m - \varepsilon_{m-1} \tilde{\mathbf{1}}) \mathbf{C}_{m-1} \\ &= \tilde{\varepsilon}_m \mathbf{F}_m + \beta_m (\tilde{\varepsilon}_m \tilde{\mathbf{N}}_m - \varepsilon_m \tilde{\mathbf{1}}) \mathbf{C}_m. \end{aligned} \quad (\text{A18})$$

Eliminating  $\mathbf{C}_{m-1}$  or  $\mathbf{F}_{m-1}$  from Eqs. (A17) and (A18) gives Eq. (2.21) or Eq. (2.22), respectively.

- 
- <sup>1</sup>J. Wiggins, E. E. Carpenter, and C. J. O'Connor, *J. Appl. Phys.* **87**, 5651 (2000).  
<sup>2</sup>T. Katayama, H. Awano, and Y. Nishihara, *J. Phys. Soc. Jpn.* **55**, 2539 (1986).  
<sup>3</sup>H. Raether, *Excitation of Plasmons and Interband Transitions by Electrons* (Springer-Verlag, Berlin, 1980), p. 116.  
<sup>4</sup>H. Raether, *Surface Plasmons on Smooth and Rough Surfaces and on Gratings* (Springer-Verlag, Berlin, 1988).  
<sup>5</sup>W. Steinmann, *Phys. Status Solidi* **28**, 437 (1968).  
<sup>6</sup>P. E. Ferguson, O. M. Stafsudd, and R. F. Wallis, *Physica B & C* **89**, 91 (1977).  
<sup>7</sup>P. M. Hui and D. Stroud, *Appl. Phys. Lett.* **50**, 950 (1987).  
<sup>8</sup>V. A. Kosobukin, *Surf. Sci.* **406**, 32 (1998).  
<sup>9</sup>V. A. Kosobukin, *Solid State Commun.* **101**, 497 (1997).  
<sup>10</sup>V. A. Kosobukin, *J. Magn. Magn. Mater.* **153**, 397 (1996).  
<sup>11</sup>G. Tessier and P. Beauvillain, *Appl. Surf. Sci.* **164**, 175 (2000).  
<sup>12</sup>T. V. Murzina, T. V. Misuryaev, A. F. Kravets, J. Gdde, D. Schuhmacher, G. Marowsky, A. A. Nikulin, and O. A. Aktsipetrov, *Surf. Sci.* **482-485**, 1101 (2001).  
<sup>13</sup>S. Kawata, *Near-Field Optics and Surface Plasmon Polaritons* (Springer-Verlag, Berlin, 2001).  
<sup>14</sup>O. A. Aktsipetrov, E. M. Dubinina, S. S. Elovikov, E. D. Mishina, A. A. Nikulin, N. N. Novikova, and M. S. Strebkov, *Solid State Commun.* **70**, 1021 (1989).  
<sup>15</sup>S. L. McCall, P. M. Platzman, and P. A. Wolff, *Phys. Lett.* **77A**, 381 (1980).  
<sup>16</sup>J. Gersten and A. Nitzan, *J. Chem. Phys.* **73**, 3023 (1980).  
<sup>17</sup>P. V. Kamat, M. Flumiani, and A. Dawson, *Colloids Surf., A* **202**, 269 (2002).  
<sup>18</sup>J. Homola, S. S. Yee, and G. Gauglitz, *Sens. Actuators B* **54**, 3 (1999).  
<sup>19</sup>W. Lukosz, *Biosens. Bioelectron.* **12**, 175 (1997).  
<sup>20</sup>U. Kreibig and P. Zacharias, *Z. Phys.* **231**, 128 (1970).  
<sup>21</sup>C. G. Granqvist and O. Hunderi, *Phys. Rev. B* **16**, 3513 (1977).  
<sup>22</sup>G. A. Niklasson and C. G. Granqvist, *J. Appl. Phys.* **55**, 3382 (1984).  
<sup>23</sup>T. K. Xia, P. M. Hui, and D. Stroud, *J. Appl. Phys.* **67**, 2736 (1990).  
<sup>24</sup>M. Inoue, *Phys. Rev. B* **36**, 2852 (1987).  
<sup>25</sup>P. Royer, J. P. Goudonnet, R. J. Warmack, and T. L. Ferrell, *Phys. Rev. B* **35**, 3753 (1987).  
<sup>26</sup>J. C. Maxwell Garnett, *Philos. Trans. R. Soc. London* **203**, 385 (1904).  
<sup>27</sup>D. A. G. Bruggeman, *Ann. Phys. (Leipzig)* **24**, 636 (1935).  
<sup>28</sup>C. G. Granqvist and O. Hunderi, *Z. Phys. B* **30**, 47 (1978).  
<sup>29</sup>C. A. Murray, *J. Opt. Soc. Am. B* **2**, 1330 (1985).  
<sup>30</sup>G. Mie, *Ann. Phys. (Paris)* **25**, 377 (1908).  
<sup>31</sup>U. Kreibig and M. Vollmer, *Optical Properties of Metal Clusters* (Springer, Berlin, 1995), pp. 15–31, 134, and 141.  
<sup>32</sup>U. Kreibig, B. Schmitz, and H. D. Breuer, *Phys. Rev. B* **36**, 5027 (1987).  
<sup>33</sup>M. Kerker, D. S. Wang, and H. Chew, *Appl. Opt.* **19**, 4159 (1980).  
<sup>34</sup>B. J. Messinger, K. Ulrich von Raben, R. K. Chang, and P. W. Barber, *Phys. Rev. B* **24**, 649 (1981).  
<sup>35</sup>A. Wokaun, *Mol. Phys.* **56**, 1 (1985).  
<sup>36</sup>M. Kerker and C. G. Blatchford, *Phys. Rev. B* **26**, 4052 (1982).  
<sup>37</sup>P. Barnickel and A. Wokaun, *Mol. Phys.* **67**, 1355 (1989).  
<sup>38</sup>S. Remita, G. Picq, J. Khatouri, and M. Mostafavi, *Radiat. Phys. Chem.* **54**, 463 (1999).  
<sup>39</sup>J. Sinzig and M. Quinten, *Appl. Phys. A: Solids Surf.* **58**, 157 (1994).  
<sup>40</sup>P. H. Lissberger and P. W. Saunders, *Thin Solid Films* **34**, 323 (1976).  
<sup>41</sup>R. Carey, D. M. Newman, and P. Bouvier, *IEEE Trans. Magn.* **33**, 3256 (1997).  
<sup>42</sup>M. Abe, *Phys. Rev. B* **53**, 7065 (1996).  
<sup>43</sup>L. D. Landau, E. M. Lifshitz, and L. P. Pitaevskii, *Electrodynamics of Continuous Media*, 2nd ed., translated by J. B. Sykes, J. S. Bell, and M. J. Kearsley (Pergamon, Oxford, 1981), p. 19.  
<sup>44</sup>J. A. Stratton, *Electromagnetic Theory* (McGraw-Hill, New York, 1941), pp. 34, 48, and 207.  
<sup>45</sup>K. U. Ingard, *Fundamentals of Waves & Oscillations* (Cambridge University Press, New York, 1988), p. 113.  
<sup>46</sup>J. G. Mavroides, in *Optical Properties of Solids*, edited by F. Abeles (North-Holland, Amsterdam, 1972), p. 357.  
<sup>47</sup>M. Abe and J. Kuroda, *J. Appl. Phys.* **91**, 7305 (2002).  
<sup>48</sup>M. Abe and J. Kuroda, to be presented at the MMM Conf., Jacksonsville, 7–11 Nov. 2004.  
<sup>49</sup>U. Kreibig, A. Althoff, and H. Pressmann, *Surf. Sci.* **106**, 308 (1981).  
<sup>50</sup>H. Frhlich, *Theory of Dielectrics: Dielectric Constant and Dielectric Loss*, 2nd ed. (Oxford University Press, London, 1986).  
<sup>51</sup>R. Landauer, *Electrical Transport and Optical Properties of Inhomogeneous Media*, edited by J. C. Garland and D. B. Tanner, AIP Conf. Proc. No. 40 (AIP, New York, 1978), p. 2.